

Sediment supply explains long-term and large-scale patterns in saltmarsh lateral expansion and erosion

Ladd, C.J.T.; Duggan Edwards, Mollie F.; Bouma, Tjeerd J.; Pages, Jordi F.; Skov, Martin W.

Geophysical Research Letters

DOI:
[10.1029/2019GL083315](https://doi.org/10.1029/2019GL083315)

Published: 28/10/2019

Peer reviewed version

[Cyswllt i'r cyhoeddiad / Link to publication](#)

Dyfyniad o'r fersiwn a gyhoeddwyd / Citation for published version (APA):

Ladd, C. J. T., Duggan Edwards, M. F., Bouma, T. J., Pages, J. F., & Skov, M. W. (2019). Sediment supply explains long-term and large-scale patterns in saltmarsh lateral expansion and erosion. *Geophysical Research Letters*, 46(20), 11178-11187.
<https://doi.org/10.1029/2019GL083315>

Hawliau Cyffredinol / General rights

Copyright and moral rights for the publications made accessible in the public portal are retained by the authors and/or other copyright owners and it is a condition of accessing publications that users recognise and abide by the legal requirements associated with these rights.

- Users may download and print one copy of any publication from the public portal for the purpose of private study or research.
- You may not further distribute the material or use it for any profit-making activity or commercial gain
- You may freely distribute the URL identifying the publication in the public portal ?

Take down policy

If you believe that this document breaches copyright please contact us providing details, and we will remove access to the work immediately and investigate your claim.

Sediment supply explains long-term and large-scale patterns in saltmarsh lateral expansion and erosion

Cai J. T. Ladd^{1,2}, Mollie F. Duggan-Edwards¹, Tjeerd J. Bouma³, Jordi F. Pagès⁴,
Martin W. Skov¹

¹School of Ocean Sciences, Bangor University, Menai Bridge, LL59 5AB, UK.

²Department of Geography, Swansea University, Swansea, SA2 8PP, UK.

³Department of Estuarine and Delta Systems, Royal Netherlands Institute for Sea Research (NIOZ), Utrecht University, 4400 AC Yerseke, P.O. Box 140, The Netherlands.

⁴Centre d'Estudis Avançats de Blanes (CEAB-CSIC), Blanes, 17300, Catalonia (Spain).

Corresponding author: C. Ladd (c.ladd@bangor.ac.uk)

Key Points:

- Sea level rise alone does not explain marsh lateral changes over the past 150 years
- Sediment flux is by far the strongest indicator of long-term lateral changes in saltmarsh extent.
- Small increases in fetch length may boost marsh expansion through stimulating wind-driven sediment transport onto marshes

Abstract

Salt marshes often undergo rapid changes in lateral extent, the causes of which lack common explanation. We combine hydrological, sedimentological and climatological data with analysis of historical maps and photographs to show that long-term patterns of lateral marsh change can be explained by large-scale variation in sediment supply and its wave-driven transport. Over 150 years, northern marshes in Great Britain expanded while most southern marshes eroded. The cause for this pattern was a north to south reduction in sediment flux and fetch-driven wave sediment resuspension and transport. Our study provides long-term and large-scale evidence that sediment supply is a critical regulator of lateral marsh dynamics. Current global declines in sediment flux to the coast are likely to diminish the resilience of salt marshes and other sedimentary ecosystems to sea level rise. Managing sediment supply is not commonplace, but may be critical to mitigating coastal impacts from climate change.

Plain Language Summary

Salt marshes are valuable ecosystems for human societies, and are especially vulnerable to losses caused by human activity and climate change. Little is known about how the size of marshes has changed in response to disturbance over large- and long-term scales. We used historical maps and aerial photographs to capture 150 years of change in marsh area extent in 25 estuaries and ~100 marshes across Great Britain. We then related the rates of marsh change to existing data on hydrology, biology, climate, sediment supply and other variables, to find out which elements best explained patterns of erosion and expansion for the period between 1967 and 2016. We found a shift from long-term marsh erosion in the south-east, to long-term marsh expansion in the north-west of Great Britain, and that this pattern was explained by a south-to-north gradient of increasing sediment flux into marshes and wave fetch lengths which

helps transport sediment onto marshes. Our study demonstrates how sediment supply should be monitored and managed to preserve saltmarsh extent into the future.

1 Introduction

The threat of sea level rise has dominated theoretical and empirical saltmarsh research for more than thirty years, from concerns that over 90% of global marshes could drown by 2100 (Crosby et al., 2016; Spencer et al., 2016; Horton et al., 2018; Valiela et al., 2018). Recent results show that marshes are adept at keeping pace with sea level rise by growing vertically when sediment is available to settle onto the marsh surface (Kirwan et al., 2016a); an irony, given that fear of marsh loss by drowning has had an overriding influence on conservation policy since the 1970s (Hatvany et al., 2015). Despite the vertical resilience to sea level rise, there are many documented cases from Europe, North America and Asia where marshes have undergone extensive lateral changes in cover, expanding or eroding hundreds of metres in just a few years (Yang et al., 2001; Lotze et al., 2006; Fagherazzi et al., 2013; Gunnell et al., 2013; Leonardi et al., 2016). This study heeds the call to investigate the drivers causing lateral marsh change (Kirwan et al., 2016a; Kirwan et al., 2016b; Schuerch et al., 2018), shifting the current emphasis away from a predominant focus on vertical growth dynamics alone (Mariotti & Fagherazzi, 2010; Kirwan et al., 2016b). The causes for lateral marsh change need to be understood if natural coastal protection by marshes is to be effectively managed (Bouma et al., 2014; Kirwan et al., 2016b; Ganju, 2019).

Marsh loss by lateral retreat is thought to be the consequence of wind-wave attack (Mariotti & Fagherazzi, 2010, 2013; Marani et al., 2011; Mariotti & Carr, 2014). Sea level rise and increased severity of storm and river flooding collectively act to raise water depths and wave/current scour over tidal flats, thereby increasing the likelihood of initiating lateral marsh erosion (Mariotti & Fagherazzi, 2010; Mariotti & Carr, 2014; Hu et al., 2015b). Previous studies have indicated that sediment supply from marine or riverine sources can diminish this erosion risk when the replenishment of sediment is sufficiently large to cause tidal flats to elevate through accretion. For example, marshes in the macrotidal Bay of Fundy, Canada, are resilient to erosion because new sources of sediment from ice rafting are transported to the saltmarsh edge by large-amplitude tides (van Proosdij et al., 2006). In contrast, some marshes in the microtidal Venice Lagoon, Italy, are erosion-prone because of low river sediment supply, as well as limited tide-driven sediment mobilisation and transport (Day et al., 1999; Marani et al., 2007; Fagherazzi et al., 2013). Along sediment-starved coastlines, erosion of adjacent tidal flats can provide a local sediment source for marsh accretion (Schuerch et al., 2019) even if tidal flat loss eventually exposes marshes to long-term lateral erosion (Bouma et al., 2016). Marsh change is also associated with human activity. Land reclamation has reduced the extent of marshes globally (Gedan et al., 2009), while the introduction of invasive marsh building plants (*Spartina* species) has expanded marshes (Ranwell, 1967; Gedan et al., 2009). Large fluctuations in marsh cover have also been linked to changes in hydrology and sediment transport driven by coastal development and land-use change (Yang et al., 2001).

While numerical models have pioneered the mechanistic understanding of lateral marsh dynamics (Mariotti & Fagherazzi, 2010; Mariotti & Carr, 2014; Hu et al., 2015a; D'Alpaos & Marani, 2016; Kirwan et al., 2016b; Schuerch et al., 2018), empirical evidence has lagged behind and been limited to process-based studies (Feagin et al., 2009; Francalanci et al., 2013), isolated sites (Chauhan, 2009; Gunnell et al., 2013; McLoughlin et al., 2014) and single explanatory drivers of change (Weston, 2013; Gabler et al., 2017). We aimed to change this

situation. Here we ask which key climate, biotic, and anthropogenic drivers best explain long-term (150-year), large-scale (across Great Britain) lateral marsh change.

2 Methods

2.1 Study sites

We measured change in saltmarsh extent for 25 estuaries and embayments located in 6 regions across Great Britain (GB): the Solway, Morecambe and Cardigan regions located along the west coast, in the Irish Sea; and the Wash, Essex-Kent and Solent regions along the east/south-east, in the North Sea and English Channel (Figure 1). In total, these estuaries occupied around 19,000 ha of salt marsh (~40% of the total marsh area in GB) (Phelan et al., 2011; Haynes, 2016). Estuaries were shallow, generally well-mixed with semidiurnal meso- to macro-tidal ranges. Flood-dominance was common along the west coast, the Wash region and many of the Essex-Kent regions, whereas in the Solent region, all the estuaries were ebb-dominant (Manning & Whitehouse, 2012). Typical estuary morphology ranged from bar-built to embayment/coastal plains (Pye & Blott, 2014). Relative sea level rise (RSLR) generally increases along an axis from the north-west to the south-east due to isostatic adjustment of the British Isles following deglaciation at the end of the Last Glacial Maximum (Bradley et al., 2009). Along a similar axis, tidal amplitude and estuary depth generally decrease, and sediment type changes from sand- to silt/clay-dominance (Goudie, 2013). All regions have historically seen some sea wall construction, with extensive stepwise reclamation occurring in the Wash and the Essex-Kent regions (Davidson et al., 1991). Fluvial suspended sediment supply to the coastline across the UK has been historically low (Worrall et al., 2013).

2.2 Change in saltmarsh extent

We quantified saltmarsh area for the entirety of each estuary approximately every 30 years between 1846 and 2016 using a combination of Ordnance Survey (OS) maps and aerial photographs. OS maps were accessed via the EDINA Digimap Resource Centre. Survey dates of maps were taken from Oliver (2013) and used as timestamps. For the Cardigan regions, aerial photographs were taken from the Royal Commission on Ancient Historical Monuments Wales. Photographs were scanned and georeferenced onto OS 1:25,000 rasters in the British National Grid projection. Pixel size corresponded to ca. 0.25×0.25 m in the field. Marsh extent measurements for the Solent and Essex-Kent regions, originally delineated from aerial photographs, were taken from Baily and Pearson (2007) and Cooper et al. (2001) respectively.

Marsh extent from OS maps and aerial photographs were delineated manually at a scale of 1:7,500 by placing vertices along the marsh edge approximately every 5 m. To account for boundary precision of the seaward marsh edge, visual comparisons between our georeferenced images to reference shapefiles (Phelan et al., 2011; Haynes, 2016) was done to ensure accuracy of the georeferencing procedure. We also looked for site-specific literature to verify whether observations of significant change in marsh extent could be considered ‘real’ or were likely caused by differences in map surveyors’ interpretation of where the marsh edge lay (see supporting information, Table S1). In the case of the Wash, large areas of marshland were reclaimed over the study period. To account for this, we calculated the area of reclaimed land and subtracted it from the marsh extent in the previous map revision. The new value was included as an additional measurement of marsh area between map revisions. See supporting information, Text S1, for methods used to calculate an error term for each measure of marsh area.

A linear rate of saltmarsh change per year was calculated for each estuary and used as the response variable in statistical modelling. Due to the highly non-linear change of marsh extent in the Wash region, an average rate of marsh change was calculated following each reclamation phase. See supporting information, Table S2, for the rates of marsh change, and the dates over which this rate was taken. We also contrasted observed rates of lateral marsh change with published empirical measurements of vertical accretion on the nearby marsh surface. All accretion rates were measured in the low-marsh zone using Caesium radio-isotope dating, Sediment Elevation Tables or Marker Horizons (see references in Table 1). See supporting information, Table S2, for dates over which accretion rates were measured.

2.3 Predictor variables of lateral marsh change

For each estuary, we collated data on key hydrological, sedimentological and climatological variables known to structure saltmarsh extent within estuaries. Annual net sediment flux per unit area of marsh was calculated by using the ratio of vegetated and unvegetated surfaces within each estuarine marsh complex (UVVR), which has been shown to be a proxy for external sediment supply (Ganju et al., 2017). See supporting information, Text S2, for information on how net sediment flux was calculated and validated. Estimated bedload sediment flux volume (in or out of the estuary) were taken from HR Wallingford (2002), Brown and Davies (2010), Halcrow (2010), and NFDC (2017). Due to differences in the precision of modelled bedload sediment flux estimates between studies, all values were rounded to their nearest 10th value, representing a magnitude flux either into (positive) or out (negative) at the estuary mouth. Long-term tide gauge records were used to calculate the rate of RSLR for each estuary. Trends of RSLR are linear rates calculated from monthly-averaged records with a minimum 30-year timespan (NOAA, 2019). Where nearby tide gauges were unavailable, we took the average RSLR rate from two nearest equidistant stations. Admiralty Tide Tables were used to determine the mean tidal range of each estuary, taken from Manning and Whitehouse (2012). Frequency of storm events were calculated using daily averaged wind speed data from the UK Met Office Integrated Data Archive System (Met Office, 2012). Stations were selected based on their proximity to each estuary. The temporal range for each station varied considerably, although at most limited to between 1957 and 2016. As a consequence, some stations nearby had low number of samples and were rejected for further analysis. The final representation of stations was limited to one per region, and storm events recorded by that station were assumed to be representative of all estuaries for the respective region. Prior to analysis, wind speed data was screened for quality and completeness (see Watson et al. (2015) for method). Frequency of storm events were then estimated from annual datasets as a count above an absolute threshold of 23 ms⁻¹ ('strong gale' on the Beaufort scale), and rate of change in number of events per year was used in the statistical analysis. Prevailing wind directions within 10-degree compass bearing intervals of each station were also used to calculate fetch length of each estuary (the distance over which wave-generating winds blow). The Waves Toolbox for ArcGIS 10.1 (Rohweder et al., 2012) with an 'SPM-Restricted' method was used to calculate fetch length every 200 m along the seaward marsh edge of each estuary (using a national marsh shapefile taken from Phelan et al. (2011) and Haynes (2016)). The median fetch lengths for each estuary were recorded. Rate change in river flood frequency events were calculated using number of Peaks-Over-Threshold per water year data provided by the National River Flow Archive (Robson and Reed, 1999). Predictor variables, and the timescale over which they were measured, are noted in supporting information, Table S2. Dates of *Spartina townsendii* and *Spartina anglica* (henceforth *Spartina spp.*) colonisation (Figure 2; grey shading) were taken from Goodman et al. (1959), Hubbard and Stebbings (1967), and Harwood and Scott (1999). Information on significant infrastructure projects (Figure 2; arrows) were

taken from Kestner (1962), Marshall (1962), and Burd (1992) for the Solway, Wash and Essex-Kent regions.

2.4 Statistical treatment

All statistical analyses were implemented in R. Predictor variables were checked for outliers, and log- or cube-transformed to meet assumptions of normality and equal variance. Predictor variables were also checked for collinearity, and dropped if Variance Inflation Factors exceeded 3 (Zuur et al., 2009). To identify groupings across our study sites, we used pairwise Euclidean distances between all 25 estuaries and found 6 clearly defined regions (Figure 1). We then used region as a random variable to test for spatial autocorrelation, but did not find a significant effect. A Stepwise Linear Regression model was therefore used to select the minimal adequate model. See supporting information, Text S3, for details on the full statistical analysis used.

4 Results and Discussion

Our analysis of marsh extent change revealed a stronger tendency for seaward lateral marsh expansion than for marsh erosion. Five of the six regions increased in marsh cover by 29% to 158% between 1846 and 2016 (Figures 2a–e and 2h) and marshes overall expanded by 11%. South-east Britain was the only region to consistently lose marsh cover (Figures 2f and 2g). The largest lateral expansion occurred in the south, where Solent marshes had grown 307% by the 1970s before declining to their current levels; 29% greater than in 1868 (Figures 2d and 2h). The north-eastern Wash region lost large areas of salt marsh on four occasions due to land reclamation (Figure 2e; arrows), however new marshes always expanded laterally on the seaward side of walls, leading to a 52% overall increase in marsh area.

Effects of *Spartina* colonisation on long-term marsh change appeared to be limited. In estuaries where marsh areal extent had been increasing, trends of marsh expansion generally preceded the arrival of invasive *Spartina* (Figures 2a–c; grey shading), with the exception of the Solent region (Figures 2d and 2h; grey shading), where *Spartina* invasion has been substantial (Hubbard, 1965). Causes for erosion post-1970 in the Solent are unclear (Baily & Pearson, 2007), however studies have reported marsh loss through lateral marsh erosion which indicates losses may be related to dynamics at the salt marsh- tidal flat interface (Johnson, 2000). In the Essex-Kent region, eroding marshes saw a prolonged period of little marsh change between 1900 and 1970 during which *Spartina* was first recorded and several sea walls were breached by storms (Figures 2f and 2g; grey bars and white arrows). Overall, coastal works also had little effect on long-term marsh change. In the Wash and Solway regions, marshes expanded despite losses through reclamation (Figure 2e; black arrows) and canalisation (Figure 2a; grey arrows) respectively. The prevailing hydrological and sedimentological environment appeared to be conducive to achieving a new dynamic equilibrium in marsh extent (Kestner, 1975). Both the effects of the introduction of *Spartina* and coastal works appear to have only temporarily offset a long-term trend of marsh decline. We therefore conclude that long-term patterns of marsh lateral change were not driven by direct human impact alone.

We next considered which key drivers were responsible for lateral marsh change for the period between 1967 and 2016. Results from a Stepwise Linear Regression model showed that sediment flux per unit area and median fetch length in combination best explained (62% of variation) the rate of marsh lateral change in estuaries across Great Britain (Table S3). Marshes shifted from eroding to expanding when sediment flux and fetch length concurrently increased

(Figure 3). Bedload sediment flux was retained in the best fit model, but was not significant (Table S3).

From a range of key hydrological, sedimentological and climatological variables known to influence lateral marsh dynamics, we find that sediment supply plays a crucial role in explaining large-scale, long-term trends of lateral marsh change (Figure 3a). Whilst increases in fetch length are typically associated with marsh loss rather than expansion (Callaghan et al., 2010), the relatively sheltered meso- to macro-tidal estuaries in our study had small fetch lengths (averaging 1.2 km) compared to the ~10 km threshold fetch lengths needed to trigger runaway marsh erosion along microtidal U.S. coastlines (Mariotti & Fagherazzi, 2013). Since wave action is also responsible for sediment resuspension and transport (Green & Coco, 2014), it is likely that moderate increases in fetch length enhances sediment transport to the coast, thereby facilitating marsh accretion (Figure 3b) as observed along other macro-tidal coastlines (Pringle, 1995; van de Groot et al., 2011). Across Great Britain, marshes with larger wave fetch lengths also tended to have longer foreshore widths (Taylor et al., 2002). The presence of a wide foreshore can attenuate incoming waves, reducing the potential for marsh edge erosion (Bouma et al., 2014 and references therein). Additional field-based measurements would be required to ascertain whether a shift from marsh erosion to expansion across Great Britain is primarily influenced by increased wave-driven sediment transport to the coast, or greater wave-protection from wider foreshores. Nevertheless, our results provide empirical support for large-scale and long-term shifts in the lateral extent of marshes driven by sediment supply and transport, in agreement with numerical models (Mariotti & Fagherazzi, 2010).

Global declines in sediment supply to the coast could lead to large-scale marsh loss through lateral erosion, as observed along the eastern U.S. coast (Weston, 2013). A spatial shift over the 1967-2013 period, from marsh complexes with a positive sediment flux to marshes that have been exporting sediment (Figure 3a) implies there might have been differences in sediment availability across Great Britain. There is no evidence that fluvial suspended sediment flux to the UK coast has changed since 1974 (Worrall et al., 2013) and there is also no indication that marine sediment sources have depleted over the past 50 years (HR Wallingford, 2002; Halcrow, 2010; NFDC, 2017). Intertidal flats, which can provide a local sediment source for marsh accretion (Mariotti & Carr, 2014; Schuerch et al., 2019), have reduced in size across GB since 1843 (Taylor et al., 2004; Pontee, 2011). More severe reductions in tidal flat widths along south and eastern England (Taylor et al., 2004) may have impaired their capacity to supply marshes with enough sediment to keep pace with sea level rise, exposing the marsh edge to long-term lateral erosion (Figure 2d and 2f-h). Estuaries with a greater capacity for sediment remobilisation and transport by wave action (Figure 3b) may have allowed marshes to continue to expand at the expense of tidal flat erosion (Figure 2a-c and 2e). Without increases in sediment supply to the coast, trends of lateral marsh erosion are likely to continue (Figure 2d and 2f-h) and may reverse trends of marsh expansion currently observed in the northern regions of Great Britain (Figure 2a-c and 2e).

Given that studies of marsh stability have tended to focus on whether or not vertical growth is equal to or greater than local sea level rise (Crosby et al., 2016; Kirwan et al., 2016a; Spencer et al., 2016; Horton et al., 2018; Schuerch et al., 2018; Valiela et al., 2018), we also compared our rates of lateral marsh change with the rates of vertical marsh accretion (references within Table 1) versus RSLR for each region. We found that all marshes had a positive accretion balance (Table 1). Marshes can erode at their flanks, but still accrete with RSLR, because lateral erosion provides a sediment source for vertical accretion (Mariotti & Carr, 2014). Coupled lateral and vertical marsh dynamics may therefore better predict saltmarsh resilience

than comparing marsh vertical growth against RSLR alone (Mariotti & Carr, 2014; Gonneea et al., 2019; Kirwan et al. 2016a; Kirwan et al. 2016b).

Schemes involving managed realignment of the coastline with engineering solutions to control sediment supply and tidal inundation can be used to build large-scale and long-term marsh resilience in historically eroding systems including San Francisco Bay, U.S.A. (Stralberg et al., 2011), and the Scheldt estuary, Netherlands (Vandenbruwaene et al., 2011). Despite such large investments into the restoration of saltmarsh flood protection, the monitoring of short-term sediment dynamics at the marsh edges (Bouma et al., 2016) and profile changes of tidal flats (Taylor et al., 2004; Pontee, 2011; Murray et al., 2014) is rarely done. This hampers the ability to predict whether marsh restoration schemes are likely to succeed or fail. Having shed light on the key drivers of long-term saltmarsh lateral change, researchers should now capitalise on advances in satellite remote sensing (Dorji et al., 2016) and novel and cheap instruments to quantify the short-term sediment dynamics at the coast (Hu et al., 2015c) to evaluate coastal resilience against human- and environment-induced change at a global scale. The evidence presented here contributes to an emerging emphasis on investigating the causes for spatial shifts in coastal systems, including mudflats (Murray et al., 2014), seagrass beds (Suykerbuyk et al., 2015) and mangroves (Gabler et al., 2017). Though important, a shift away from a focus on sea level rise alone to consider also the influences of other anthropogenic and macroclimatic drivers of coastline change should be a priority.

Acknowledgments

This research was supported by Coleg Cymraeg Cenedlaethol to C.J.T.L., by the Welsh Government and Higher Education Funding Council for Wales through Sêr Cymru National Research Network for Low Carbon, Energy and Environment to M.F.D-E, J.F.P., T.J.B. and M.W.S., by the NERC C-SIDE grant no. NE/R010846/1 to C.J.T.L. and M.W.S., and by the NWO BE-SAFE grant no. 850.13.011 and TTW AllRisk (P21.2 project B) for financial support in understanding the use of salt marshes for coastal defence to T.J.B.

We thank Prof. Tom Spencer from Cambridge University and Dr Jonathan Malarkey, Prof. Jaco Baas, Prof. Hilary Kennedy and Prof. Stuart Jenkins from Bangor University for their constructive comments.

The GIS layers showing change in marsh extent and the variables used in the statistical analysis for this study are accessible via the Environmental Information Data Centre repository (DOI: 10.5285/03b62fd0-41e2-4355-9a06-1697117f0717).

The authors declare no conflict of interest.

References

- Baily, B., & Pearson, A. W. (2007) Change detection mapping and analysis of salt marsh areas of central southern England from Hurst Castle Spit to Pagham Harbour. *Journal of Coastal Research* 23(6), 1549–1564. <https://doi.org/10.2112/05-0597.1>
- Bouma, T. J., van Belzen, J., Balke, T., Zhu, Z., Airoldi, L., Blight, A. J., et al. (2014). Identifying knowledge gaps hampering application of intertidal habitats in coastal protection: Opportunities & steps to take. *Coastal Engineering*, 87, 147–157. <https://doi.org/10.1016/j.coastaleng.2013.11.014>

- Bouma, T. J., van Belzen, J., Balke, T., van Dalen, J., Klaassen, P., Hartog, A. M., et al. (2016). Short-term mudflat dynamics drive long-term cyclic salt marsh dynamics. *Limnology and Oceanography*, 61(6), 2261–2275. <https://doi.org/10.1002/lno.10374>
- Bradley, S. L., Milne, G. A., Teferle, F. N., Bingley, R. M., & Orliac, E. J. (2009). Glacial isostatic adjustment of the British Isles: New constraints from GPS measurements of crustal motion. *Geophysical Journal International*, 178(1), 14–22. <https://doi.org/10.1111/j.1365-246x.2008.04033.x>
- Brown, J. M., & Davies, A. G. (2010). Flood/ebb tidal asymmetry in a shallow sandy estuary and the impact on net sand transport. *Geomorphology*, 114(3), 431–439. <https://doi.org/10.1016/j.geomorph.2009.08.006>
- Burd, F. (1992). *Historical study of sites of natural sea wall failures in Essex* (ENRR015). Hull: Natural England. Retrieved from <http://publications.naturalengland.org.uk/publication/33021>
- Callaghan, D. P., Bouma, T. J., Klaassen, P., van der Wal, D., Stive, M. J. F., & Herman, P. M. J. (2010). Hydrodynamic forcing on salt-marsh development: Distinguishing the relative importance of waves and tidal flows. *Estuarine, Coastal and Shelf Science*, 89(1), 73–88. <https://doi.org/10.1016/j.ecss.2010.05.013>
- Chauhan, P. P. S. (2009). Autocyclic erosion in tidal marshes. *Geomorphology*, 110(3–4), 45–57. <https://doi.org/10.1016/j.geomorph.2009.03.016>
- Cooper, N. J., Cooper, T., & Burd, F. (2001). 25 years of salt marsh erosion in Essex: Implications for coastal defence and nature conservation. *Journal of Coastal Conservation*, 7(1), 31–40. <https://doi.org/10.1007/bf02742465>
- Crosby, S. C., Sax, D. F., Palmer, M. E., Booth, H. S., Deegan, L. A., Bertness, M. D., & Leslie, H. M. (2016). Salt marsh persistence is threatened by predicted sea-level rise. *Estuarine, Coastal and Shelf Science*, 181, 93–99. <https://doi.org/10.1016/j.ecss.2016.08.018>
- Cundy, A. B., & Croudace, I. W. (1996). Sediment accretion and recent sea-level rise in the Solent, southern England: Inferences from radiometric and geochemical studies. *Estuarine, Coastal and Shelf Science*, 43(4), 449–467. <https://doi.org/10.1006/ecss.1996.0081>
- D’Alpaos, A., & Marani, M. (2016). Reading the signatures of biologic–geomorphic feedbacks in salt-marsh landscapes. *Advances in Water Resources*, 93(B), 265–275. <https://doi.org/10.1016/j.advwatres.2015.09.004>
- Davidson, N. C., Laffoley, D. d’A., Doody, J. P., Way, L. S., Gordon, J., Key, R. et al. (1991). The size of the British estuarine resource. In *Nature conservation and estuaries in Great Britain*. Peterborough: Nature Conservancy Council. Retrieved from <http://jncc.defra.gov.uk/page-2563>
- Day Jr, J. W., Rybczyk, J., Scarton, F., Rismondo, A., Are, D., & Cecconi, G. (1999). Soil accretionary dynamics, sea-level rise and the survival of wetlands in Venice Lagoon: A field and modelling approach. *Estuarine, Coastal and Shelf Science*, 49(5), 607–628. <https://doi.org/10.1006/ecss.1999.0522>
- Dorji, P., Fearn, P., & Broomhall, M. (2016). A semi-analytic model for estimating total suspended sediment concentration in turbid coastal waters of northern Western Australia using MODIS-Aqua 250 m data. *Remote Sensing*, 8(7), 556. <https://doi.org/10.3390/rs8070556>
- Fagherazzi, S., Mariotti, G., Wiberg, P., & McGlathery, K. (2013). Marsh collapse does not require sea level rise. *Oceanography*, 26(3), 70–77. <https://doi.org/10.5670/oceanog.2013.47>

371 Feagin, R. A., Lozada-Bernard, S. M., Ravens, T. M., Moller, I., Yeager, K. M., & Baird, A. H.
372 (2009). Does vegetation prevent wave erosion of salt marsh edges? *Proceedings of the National*
373 *Academy of Sciences*, 106(25), 10109–10113. <https://doi.org/10.1073/pnas.0901297106>

374 Francalanci, S., Bondoni, M., Rinaldi, M., & Solari, L. (2013). Ecomorphodynamic evolution of
375 salt marshes: Experimental observations of bank retreat processes. *Geomorphology*, 195, 53–65.
376 <https://doi.org/10.1016/j.geomorph.2013.04.026>

377 Gabler, C. A., Osland, M. J., Grace, J. B., Stagg, C. L., Day, R. H., Hartley, S. B., et al. (2017).
378 Macroclimatic change expected to transform coastal wetland ecosystems this century. *Nature*
379 *Climate Change*, 7(3), 227–227. <https://doi.org/10.1038/nclimate3232>

380 Ganju, N. K., Defne, Z., Kirwan, M. L., Fagherazzi, S., D'Alpaos, A., & Carniello, L. (2017).
381 Spatially integrative metrics reveal hidden vulnerability of microtidal salt marshes. *Nature*
382 *Communications*, 8, 14156. <https://doi.org/10.1038/ncomms14156>

383 Ganju, N. K., Kirwan, M. L., Dickhudt, P. J., Guntenspergen, G. R., Cahoon, D. R., & Kroeger,
384 K. D. (2015). Sediment transport-based metrics of wetland stability. *Geophysical Research*
385 *Letters*, 42(19), 7992–8000. <https://doi.org/10.1002/2015gl065980>

386 Ganju, N. K. (2019). Marshes are the new beaches: Integrating sediment transport into restoration
387 planning. *Estuaries and Coasts*, 42(4), 917–926. <https://doi.org/10.1007/s12237-019-00531-3>

388 Gedan, K. B., Silliman, B. R., & Bertness, M. D. (2009). Centuries of human-driven change in
389 salt marsh ecosystems. *Annual Review of Marine Science*, 1(1), 117–141.
390 <https://doi.org/10.1146/annurev.marine.010908.163930>

391 Gonneea, M. E., Maio, C. V., Kroeger, K. D., Hawkes, A. D., Mora, J., Sullivan, R., et al. (2019).
392 Salt marsh ecosystem restructuring enhances elevation resilience and carbon storage during
393 accelerating relative sea-level rise. *Estuarine, Coastal and Shelf Science*, 217, 56–68.
394 <https://doi.org/10.1016/j.ecss.2018.11.003>

395 Goodman, P. J., Braybrooks, E. M., & Lambert, J. M. (1959). Investigations into 'Die-Back' in
396 *Spartina townsendii* AGG.: I. The present status of *Spartina townsendii* in Britain. *The Journal of*
397 *Ecology*, 47(3), 651–677. <https://doi.org/10.2307/2257297>

398 Goudie, A. (2013). Characterising the distribution and morphology of creeks and pans on salt
399 marshes in England and Wales using Google Earth. *Estuarine, Coastal and Shelf Science*, 129,
400 112–123. <https://doi.org/10.1016/j.ecss.2013.05.015>

401 Green, M. O., & Coco, G. (2014). Review of wave-driven sediment resuspension and transport in
402 estuaries. *Reviews of Geophysics*, 52(1), 77–117. <https://doi.org/10.1002/2013rg000437>

403 Gunnell, J. R., Rodriguez, A. B., & McKee, B. A. (2013). How a marsh is built from the bottom
404 up. *Geology*, 41(8), 859–862. <https://doi.org/10.1130/g34582.1>

405 Haynes, T. (2016). *Scottish saltmarsh survey national report* (Commissioned Report No. 786).
406 Inverness: Scottish Natural Heritage. Retrieved from
407 [https://www.nature.scot/sites/default/files/2017-05/Publication%202016%20-](https://www.nature.scot/sites/default/files/2017-05/Publication%202016%20-%20SNH%20Commissioned%20Report%20786%20-%20Scottish%20saltmarsh%20survey%20national%20report%20%28A2215730%29.pdf)
408 [%20SNH%20Commissioned%20Report%20786%20-](https://www.nature.scot/sites/default/files/2017-05/Publication%202016%20-%20SNH%20Commissioned%20Report%20786%20-%20Scottish%20saltmarsh%20survey%20national%20report%20%28A2215730%29.pdf)
409 [%20Scottish%20saltmarsh%20survey%20national%20report%20%28A2215730%29.pdf](https://www.nature.scot/sites/default/files/2017-05/Publication%202016%20-%20SNH%20Commissioned%20Report%20786%20-%20Scottish%20saltmarsh%20survey%20national%20report%20%28A2215730%29.pdf)

410 Halcrow. (2010). Appendix A: Regional and sub-tidal modelling (Cell Eleven Tide and Sediment
411 transport Study (CETaSS) Stage 2). In *Cell Eleven Tidal and Sediment Transport Study (CETaSS)*
412 *Phase 2 (ii): Main report – summary of findings*. Swindon: Halcrow.

- Harwood, T. R., & Scott, R. (1999). *A report on Spartina anglica control Grange-over-Sands 1998-1999 for South Lakeland District Council*. Cambridge: Institute of Terrestrial Ecology. Retrieved from <http://nora.nerc.ac.uk/id/eprint/6686/>
- Hatvany, M., Cayer, D., & Parent, A. (2015). Interpreting salt marsh dynamics: Challenging scientific paradigms. *Annals of the Association of American Geographers*, 105(5), 1041–1060. <https://doi.org/10.1080/00045608.2015.1059172>
- Horton, B. P., Shennan, I., Bradley, S. L., Cahill, N., Kirwan, M., Kopp, R. E., & Shaw, T. A. (2018). Predicting marsh vulnerability to sea-level rise using Holocene relative sea-level data. *Nature Communications*, 9(1), 2687. <https://doi.org/10.1038/s41467-018-05080-0>
- HR Wallingford. (2002). Southern North Sea sediment transport study: Phase 2. *Sediment Transport Report* (Report EX 4526). Wallingford: HR Wallingford. Retrieved from <https://www.north-norfolk.gov.uk/media/3112/southern-north-sea-sediment-transport-study-phase-2-main-report.pdf>
- Hu, Z., van Belzen, J., van der Wal, D., Balke, T., Wang, Z. B., Stive, M., & Bouma, T. J. (2015a). Windows of opportunity for salt marsh vegetation establishment on bare tidal flats: The importance of temporal and spatial variability in hydrodynamic forcing. *Journal of Geophysical Research: Biogeosciences*, 120(7), 1450–1469. <https://doi.org/10.1002/2014jg002870>
- Hu, Z., Wang, Z. B., Zitman, T. J., Stive, M. J. F., & Bouma, T. J. (2015b). Predicting long-term and short-term tidal flat morphodynamics using a dynamic equilibrium theory. *Journal of Geophysical Research: Earth Surface*, 120(9), 1803–1823. <https://doi.org/10.1002/2015jf003486>
- Hu, Z., Lenting, W., van der Wal, D., & Bouma, T. J. (2015c). Continuous monitoring bed-level dynamics on an intertidal flat: Introducing novel, stand-alone high-resolution SED-sensors. *Geomorphology*, 245, 223–230. <https://doi.org/10.1016/j.geomorph.2015.05.027>
- Hubbard, J. C. E. (1965). *Spartina* marshes in southern England: VI. Pattern of invasion in Poole Harbour. *The Journal of Ecology*, 53(3), 799–813. <https://doi.org/10.2307/2257637>
- Hubbard, J. C. E., & Stebbings, R. E. (1967) Distribution, dates of origin and acreage of *Spartina townsendii* (s.l.) marshes in Great Britain. *Proceedings of the Botanical Society of the British Isles*, 7(1), 1–7.
- Johnson, D. E. (2000). Ecological restoration options for the Lymington/Keyhaven saltmarshes. *Water and Environment Journal*, 14(2), 111–116. <https://doi.org/10.1111/j.1747-6593.2000.tb00236.x>
- Kestner, F. J. T. (1962). The old coastline of the Wash. *The Geographical Journal*, 128(4), 457–471. <https://doi.org/10.2307/1792042>
- Kestner, F. J. T. (1975). The loose-boundary regime of the Wash. *The Geographical Journal*, 141(3), 388–414. <https://doi.org/10.2307/1796474>
- Kirwan, M. L., Temmerman, S., Skeeahan, E. E., Guntenspergen, G. R., & Fagherazzi, S. (2016a). Overestimation of marsh vulnerability to sea level rise. *Nature Climate Change*, 6(3), 253–260. <https://doi.org/10.1038/nclimate2909>
- Kirwan, M. L., Walters, D. C., Reay, W. G., & Carr, J. A. (2016b). Sea level driven marsh expansion in a coupled model of marsh erosion and migration. *Geophysical Research Letters*, 43(9), 4366–4373. <https://doi.org/10.1002/2016gl068507>
- Leonardi, N., Defne, Z., Ganju, N. K., & Fagherazzi, S. (2016). Salt marsh erosion rates and boundary features in a shallow bay. *Journal of Geophysical Research: Earth Surface*, 121(10), 1861–1875. <https://doi.org/10.1002/2016jf003975>

457 Lotze, H. K. (2006). Depletion, degradation, and recovery potential of estuaries and coastal seas.
458 *Science*, 312(5781), 1806–1809. <https://doi.org/10.1126/science.1128035>

459 Manning, A. J., & Whitehouse, R. S. J. (2012). *Enhanced UK estuaries database: Explanatory*
460 *notes and metadata* (HR Wallingford Report DDY0427 – RT002-R02-00). Wallingford: HR
461 Wallingford. Retrieved from: [http://eprints.hrwallingford.co.uk/650/1/DDY0427-RT002-R02-](http://eprints.hrwallingford.co.uk/650/1/DDY0427-RT002-R02-00.pdf)
462 [00.pdf](http://eprints.hrwallingford.co.uk/650/1/DDY0427-RT002-R02-00.pdf)

463 Mariotti, G., & Carr, J. (2014). Dual role of salt marsh retreat: Long-term loss and short-term
464 resilience. *Water Resources Research*, 50(4), 2963–2974. <https://doi.org/10.1002/2013wr014676>

465 Marani, M., D’Alpaos, A., Lanzoni, S., Carniello, L., & Rinaldo, A. (2007). Biologically-
466 controlled multiple equilibria of tidal landforms and the fate of the Venice lagoon. *Geophysical*
467 *Research Letters*, 34(11). <https://doi.org/10.1029/2007gl030178>

468 Marani, M., D’Alpaos, A., Lanzoni, S., & Santalucia, M. (2011). Understanding and predicting
469 wave erosion of marsh edges. *Geophysical Research Letters*, 38(21).
470 <https://doi.org/10.1029/2011gl048995>

471 Mariotti, G., & Fagherazzi, S. (2010). A numerical model for the coupled long-term evolution of
472 salt marshes and tidal flats. *Journal of Geophysical Research*, 115(F1).
473 <https://doi.org/10.1029/2009jf001326>

474 Mariotti, G., & Fagherazzi, S. (2013). Critical width of tidal flats triggers marsh collapse in the
475 absence of sea-level rise. *Proceedings of the National Academy of Sciences*, 110(14), 5353–5356.
476 <https://doi.org/10.1073/pnas.1219600110>

477 Marshall, J. R. (1962). The morphology of the upper Solway salt marshes. *Scottish Geographical*
478 *Magazine*, 78(2), 81–99. <https://doi.org/10.1080/00369226208735859>

479 McLoughlin, S. M., Wiberg, P. L., Safak, I., & McGlathery, K. J. (2014). Rates and forcing of
480 marsh edge erosion in a shallow coastal bay. *Estuaries and Coasts*, 38(2), 620–638.
481 <https://doi.org/10.1007/s12237-014-9841-2>

482 Met Office. (2012). *Met Office Integrated Data Archive System (MIDAS) land and marine surface*
483 *stations data (1853-current)*. NCAS British Atmospheric Data Centre. Retrieved from
484 <catalogue.ceda.ac.uk/uuid/220a65615218d5c9cc9e4785a3234bd0>

485 Murray, N. J., Clemens, R. S., Phinn, S. R., Possingham, H. P., & Fuller, R. A. (2014). Tracking
486 the rapid loss of tidal wetlands in the Yellow Sea. *Frontiers in Ecology and the Environment*,
487 12(5), 267–272. <https://doi.org/10.1890/130260>

488 NFDC (New Forest District Council). (2017). *2012 update of Carter, D., Bray, M., & Hooke, J.,*
489 *2004 SCOPAC sediment transport study*. Retrieved from www.scopac.org.uk/sts

490 NOAA (National Oceanic and Atmospheric Administration). (2019). *Sea Levels Online: Sea level*
491 *variations of the United States derived from National Water Level Observation Network stations*.
492 Retrieved from <http://tidesandcurrents.noaa.gov/sltrends/sltrends.html>

493 Oliver, R. R. (2013) *Ordnance Survey maps: A concise guide for historians*. Bath: CPI Bath
494 Press.

495 Phelan, N., Shaw, A., & Baylis, A. (2011). The extent of saltmarsh in England and Wales: 2006-
496 2009. Bristol: Environment Agency. Retrieved from
497 [https://www.gov.uk/government/publications/the-extent-of-saltmarsh-in-england-and-wales-](https://www.gov.uk/government/publications/the-extent-of-saltmarsh-in-england-and-wales-2006-to-2009)
498 [2006-to-2009](https://www.gov.uk/government/publications/the-extent-of-saltmarsh-in-england-and-wales-2006-to-2009)

499 Pontee, N. I. (2011). Reappraising coastal squeeze: A case study from north-west England.
500 *Proceedings of the Institution of Civil Engineers - Maritime Engineering*, 164(3), 127–138.
501 <https://doi.org/10.1680/maen.2011.164.3.127>

502 Pringle, A. W. (1995). Erosion of a cyclic saltmarsh in Morecambe Bay, north-west England.
503 *Earth Surface Processes and Landforms*, 20(5), 387–405. <https://doi.org/10.1002/esp.3290200502>

504 Pye, K., & Blott, S. J. (2014). The geomorphology of UK estuaries: The role of geological
505 controls, antecedent conditions and human activities. *Estuarine, Coastal and Shelf Science*, 150,
506 196–214. <https://doi.org/10.1016/j.ecss.2014.05.014>

507 Ranwell, D. S. (1967). World resources of *Spartina townsendii* (*sensu lato*) and economic use of
508 *Spartina* marshland. *The Journal of Applied Ecology*, 4(1), 239–256.
509 <https://doi.org/10.2307/2401421>

510 Robson, A., & Reed, D. (1999). *Flood estimation handbook*. Wallingford: Institute of Hydrology.

511 Rohweder, J., Rogala, J. T., Johnson, B. L., Anderson, D., Clark, S., Chamberlin, F., et al. (2012)
512 Application of wind fetch and wave models for habitat rehabilitation and enhancement projects -
513 2012 update. La Crosse, Wisconsin: United States Geological Survey, Retrieved from
514 https://umesc.usgs.gov/management/dss/wind_fetch_wave_models_2012update.html.

515 Schuerch, M., Spencer, T., Temmerman, S., Kirwan, M. L., Wolff, C., Lincke, D., et al. (2018).
516 Future response of global coastal wetlands to sea-level rise. *Nature*, 561(7722), 231–234.
517 <https://doi.org/10.1038/s41586-018-0476-5>

518 Schuerch, M., Spencer, T., & Evans, B. (2019). Coupling between tidal mudflats and salt marshes
519 affects marsh morphology. *Marine Geology*, 412, 95–106.
520 <https://doi.org/10.1016/j.margeo.2019.03.008>

521 Shi, Z. (1993). Recent saltmarsh accretion and sea level fluctuations in the Dyfi estuary, central
522 Cardigan Bay, Wales, UK. *Geo-Marine Letters*, 13(3), 182–188.
523 <https://doi.org/10.1007/bf01593192>

524 Spencer, T., Schuerch, M., Nicholls, R. J., Hinkel, J., Lincke, D., Vafeidis, A. T., et al. (2016).
525 Global coastal wetland change under sea-level rise and related stresses: The DIVA Wetland
526 Change Model. *Global and Planetary Change*, 139, 15–30.
527 <https://doi.org/10.1016/j.gloplacha.2015.12.018>

528 Stralberg, D., Brennan, M., Callaway, J. C., Wood, J. K., Schile, L. M., Jongsomjit, D., et al.
529 (2011). Evaluating tidal marsh sustainability in the face of sea-level rise: A hybrid modeling
530 approach applied to San Francisco Bay. *PLoS ONE*, 6(11), e27388.
531 <https://doi.org/10.1371/journal.pone.0027388>

532 Suykerbuyk, W., Bouma, T. J., Govers, L. L., Giesen, K., de Jong, D. J., Herman, P., et al. (2015).
533 Surviving in changing seascapes: Sediment dynamics as bottleneck for long-term seagrass
534 presence. *Ecosystems*, 19(2), 296–310. <https://doi.org/10.1007/s10021-015-9932-3>

535 Taylor, J. A., Murdock, A. P., & Pontee, N. I. (2004). A macroscale analysis of coastal steepening
536 around the coast of England and Wales. *The Geographical Journal*, 170(3), 179–188.
537 <https://doi.org/10.1111/j.0016-7398.2004.00119.x>

538 Valiela, I., Lloret, J., Bowyer, T., Miner, S., Remsen, D., Elmstrom, E., et al. (2018). Transient
539 coastal landscapes: Rising sea level threatens salt marshes. *Science of The Total Environment*,
540 640–641, 1148–1156. <https://doi.org/10.1016/j.scitotenv.2018.05.235>

- van de Groot, A. V., Veeneklaas, R. M., & Bakker, J. P. (2011). Sand in the salt marsh: Contribution of high-energy conditions to salt-marsh accretion. *Marine Geology*, 282(3–4), 240–254. <https://doi.org/10.1016/j.margeo.2011.03.002>
- van der Wal, D., & Pye, K. (2004). Patterns, rates and possible causes of saltmarsh erosion in the Greater Thames area (UK). *Geomorphology*, 61(3–4), 373–391. <https://doi.org/10.1016/j.geomorph.2004.02.005>
- van Proosdij, D., Ollerhead, J., & Davidson-Arnott, R. G. D. (2006). Seasonal and annual variations in the volumetric sediment balance of a macro-tidal salt marsh. *Marine Geology*, 225(1–4), 103–127. <https://doi.org/10.1016/j.margeo.2005.07.009>
- Vandenbruwaene, W., Maris, T., Cox, T. J. S., Cahoon, D. R., Meire, P., & Temmerman, S. (2011). Sedimentation and response to sea-level rise of a restored marsh with reduced tidal exchange: Comparison with a natural tidal marsh. *Geomorphology*, 130(3–4), 115–126. <https://doi.org/10.1016/j.geomorph.2011.03.004>
- Watson, S.J., Kritharas, P., & Hodgson, G.J. (2015) Wind speed variability across the UK between 1957 and 2011. *Wind Energy*, 18(1), 21–42. <https://doi.org/10.1002/we.1679>
- Weston, N. B. (2013). Declining sediments and rising seas: An unfortunate convergence for tidal wetlands. *Estuaries and Coasts*, 37(1), 1–23. <https://doi.org/10.1007/s12237-013-9654-8>
- Worrall, F., Burt, T. P., & Howden, N. J. K. (2013). The flux of suspended sediment from the UK 1974 to 2010. *Journal of Hydrology*, 504, 29–39. <https://doi.org/10.1016/j.jhydrol.2013.09.012>
- Yang, S., Ding, P., & Chen, S. (2001). Changes in progradation rate of the tidal flats at the mouth of the Changjiang (Yangtze) River, China. *Geomorphology*, 38(1–2), 167–180. [https://doi.org/10.1016/s0169-555x\(00\)00079-9](https://doi.org/10.1016/s0169-555x(00)00079-9)
- Zuur, A. F., Ieno, E. N., Walker, N., Saveliev, A. A., & Smith, G. M. (2009). Mixed effects models and extensions in ecology with R. New York: Springer NY. <https://doi.org/10.1007/978-0-387-87458-6>

References from supporting information

- Baily, B. (2011). Tidal line surveying and Ordnance Survey mapping for coastal geomorphological research. *Survey Review*, 43(321), 252–268. <https://doi.org/10.1179/003962611x13055561708263>
- Baily, B., & Collier, P. (2010). The Development of the Photogrammetric Mapping of tidal lines by the Ordnance Survey. *The Cartographic Journal*, 47(3), 262–269. <https://doi.org/10.1179/000870410x12786821061530>
- Baily, B., & Inkpen, R. (2013). Assessing historical saltmarsh change; an investigation into the reliability of historical saltmarsh mapping using contemporaneous aerial photography and cartographic data. *Journal of Coastal Conservation*, 17(3), 503–514. <https://doi.org/10.1007/s11852-013-0250-7>
- Baily, B., & Pearson, A. W. (2007). Change detection mapping and analysis of salt marsh areas of central southern England from Hurst Castle Spit to Pagham Harbour. *Journal of Coastal Research* 23(6), 1549–1564. <https://doi.org/10.2112/05-0597.1>
- Bridson, R. (1980). Saltmarsh: Its accretion and erosion at Caerlaverock National Nature Reserve, Dumfries. *Transactions of the Dumfriesshire and Galloway Natural History and Antiquarian Society*, 55, 60–67. Retrieved at http://www.dgnhas.org.uk/card_3055-02

584 Burd, F. (1992). *Historical study of sites of natural sea wall failures in Essex* (ENRR015). Hull:
585 Natural England. Retrieved from <http://publications.naturalengland.org.uk/publication/33021>

586 CCO (Channel Coastal Observatory). (2011). *Annual local monitoring report: Solway Firth*.
587 Allerdale: Allerdale Borough Council. Retrieved from
588 https://www.channelcoast.org/northwest/latest/index.php?link=&dla=download&id=12&cat=1/Solway%20Pages%20from%20Allerdale_Monitoring_Report_2011.pdf
589

590 CH2M HILL. (2013a). *North West Estuaries Processes Reports - Leven Estuary*. Report prepared
591 by CH2M HILL for the North West and North Wales Coastal Group, August 2013. Sefton: Sefton
592 Council. Retrieved from
593 https://www.channelcoast.org/northwest/latest/index.php?link=&dla=download&id=6&cat=1/Leven_Estuary_Processes_Report_Final.pdf
594

595 CH2M HILL. (2013b). *North West Estuaries Processes Reports - Kent Estuary*. Report prepared
596 by CH2M HILL for the North West and North Wales Coastal Group, August 2013. Sefton: Sefton
597 Council. Retrieved from
598 http://www.channelcoast.org/northwest/latest/index.php?link=&dla=download&id=5&cat=1/Kent_Estuary_Processes_Report_Final.pdf
599

600 CH2M HILL. (2013c). *North West Estuaries Processes Reports - Duddon Estuary*. Report
601 prepared by CH2M HILL for the North West and North Wales Coastal Group, August 2013.
602 Sefton: Sefton Council. Retrieved from
603 https://www.channelcoast.org/northwest/latest/index.php?link=&dla=download&id=4&cat=1/Duddon_Estuary_Processes_report_Final.pdf
604

605 Chater, E. H., & Jones, H. (1957). Some observations on *Spartina townsendii* H. and J. Groves in
606 the Dovey estuary. *The Journal of Ecology*, 45(1), 157–167. <https://doi.org/10.2307/2257082>

607 Cooper, N. J., Cooper, T., & Burd, F. (2001). 25 years of salt marsh erosion in Essex:
608 Implications for coastal defence and nature conservation. *Journal of Coastal Conservation*, 7(1),
609 31–40. <https://doi.org/10.1007/bf02742465>

610 Dixon-Gough, R. W. (2006). Changes in land use and their implications upon coastal regions:
611 The case of Grange-over-Sands, northwest England. In R. W. Dixon-Gough, P.C. Bloch (Eds.),
612 *The role of the state and individual in sustainable land management, Land Degradation and*
613 *Development Series* (Vol. 20, Issue 2, pp. 14–31). Aldershot: Ashgate Publishing Ltd.

614 FGDC (Federal Geographic Data Committee). (1998). *Geospatial positioning accuracy*
615 *standards, part 3: National standard for spatial data accuracy* (FGDC-STD-007.3-1998).
616 Washington, DC: U.S. Geological Survey. Retrieved from
617 https://www.fgdc.gov/standards/projects/accuracy/part3/index_html

618 Firth, C. R., Collins, P. E., & Smith, D. E. (2000). *Focus on firths: Coastal landforms, processes*
619 *and management options; V: The Solway Firth*. Iselworth: Scottish National Heritage.

620 Ganju, N. K., Defne, Z., Kirwan, M. L., Fagherazzi, S., D'Alpaos, A., & Carniello, L. (2017).
621 Spatially integrative metrics reveal hidden vulnerability of microtidal salt marshes. *Nature*
622 *Communications*, 8, 14156. <https://doi.org/10.1038/ncomms14156>

623 Ganju, N. K., Kirwan, M. L., Dickhudt, P. J., Guntenspergen, G. R., Cahoon, D. R., & Kroeger,
624 K. D. (2015). Sediment transport-based metrics of wetland stability. *Geophysical Research*
625 *Letters*, 42(19), 7992–8000. <https://doi.org/10.1002/2015gl065980>

626 Gray, A. J. (1972). The ecology of Morecambe Bay. V. The salt marshes of Morecambe Bay. *The*
627 *Journal of Applied Ecology*, 9(1), 207–220. <https://doi.org/10.2307/2402057>

628 Haynes, T. (2016). *Scottish saltmarsh survey national report* (Commissioned Report No. 786).
629 Inverness: Scottish Natural Heritage. Retrieved from
630 [https://www.nature.scot/sites/default/files/2017-05/Publication%202016%20-](https://www.nature.scot/sites/default/files/2017-05/Publication%202016%20-%20SNH%20Commissioned%20Report%20786%20-%20Scottish%20saltmarsh%20survey%20national%20report%20%28A2215730%29.pdf)
631 [%20SNH%20Commissioned%20Report%20786%20-](https://www.nature.scot/sites/default/files/2017-05/Publication%202016%20-%20SNH%20Commissioned%20Report%20786%20-%20Scottish%20saltmarsh%20survey%20national%20report%20%28A2215730%29.pdf)
632 [%20Scottish%20saltmarsh%20survey%20national%20report%20%28A2215730%29.pdf](https://www.nature.scot/sites/default/files/2017-05/Publication%202016%20-%20SNH%20Commissioned%20Report%20786%20-%20Scottish%20saltmarsh%20survey%20national%20report%20%28A2215730%29.pdf)

633 HMLR (Her Majesty's Land Registry). (2016). *HM Land Registry plans: The basis of HM Land*
634 *Registry applications* (PG40s1) London: Her Majesty's Land Registry. Retrieved from
635 [www.gov.uk/government/publications/land-registry-plans-the-basis-of-land-registry-](http://www.gov.uk/government/publications/land-registry-plans-the-basis-of-land-registry-applications/land-registry-plans-the-basis-of-land-registry-plans-practice-guide-40-supplement-1)
636 [applications/land-registry-plans-the-basis-of-land-registry-plans-practice-guide-40-supplement-1.](http://www.gov.uk/government/publications/land-registry-plans-the-basis-of-land-registry-applications/land-registry-plans-the-basis-of-land-registry-plans-practice-guide-40-supplement-1)

637 HR Wallingford. (2002). Southern North Sea sediment transport study: Phase 2. *Sediment*
638 *Transport Report* (Report EX 4526). Wallingford: HR Wallingford. Retrieved from
639 [https://www.north-norfolk.gov.uk/media/3112/southern-north-sea-sediment-transport-study-](https://www.north-norfolk.gov.uk/media/3112/southern-north-sea-sediment-transport-study-phase-2-main-report.pdf)
640 [phase-2-main-report.pdf](https://www.north-norfolk.gov.uk/media/3112/southern-north-sea-sediment-transport-study-phase-2-main-report.pdf)

641 Jenny, B., & Hurni, L. (2011). Studying cartographic heritage: Analysis and visualization of
642 geometric distortions. *Computers & Graphics*, 35(2), 402–411.
643 <https://doi.org/10.1016/j.cag.2011.01.005>

644 Jongepier, I., Soens, T., Temmerman, S., & Missiaen, T. (2016). Assessing the planimetric
645 accuracy of historical maps (sixteenth to nineteenth centuries): New methods and potential for
646 coastal landscape reconstruction. *The Cartographic Journal*, 53(2), 114–132.
647 <https://doi.org/10.1179/1743277414y.00000000095>

648 Kestner, F. J. T. (1962). The old coastline of the Wash. *The Geographical Journal*, 128(4), 457–
649 471. <https://doi.org/10.2307/1792042>

650 Kestner, F. J. T. (1975). The loose-boundary regime of the Wash. *The Geographical Journal*,
651 141(3), 388–414. <https://doi.org/10.2307/1796474>

652 Kirby, R. (2013). The long-term sedimentary regime of the outer Medway estuary. *Ocean and*
653 *Coastal Management*, 79, 20–33. <https://doi.org/10.1016/j.ocecoaman.2012.05.028>

654 Kirwan, M. L., Temmerman, S., Skeeahan, E. E., Guntenspergen, G. R., & Fagherazzi, S. (2016).
655 Overestimation of marsh vulnerability to sea level rise. *Nature Climate Change*, 6(3), 253–260.
656 <https://doi.org/10.1038/nclimate2909>

657 Manning, A. J., & Whitehouse, R. S. J. (2012). *Enhanced UK estuaries database: Explanatory*
658 *notes and metadata* (HR Wallingford Report DDY0427 – RT002-R02-00). Wallingford: HR
659 Wallingford. Retrieved from: [http://eprints.hrwallingford.co.uk/650/1/DDY0427-RT002-R02-](http://eprints.hrwallingford.co.uk/650/1/DDY0427-RT002-R02-00.pdf)
660 [00.pdf](http://eprints.hrwallingford.co.uk/650/1/DDY0427-RT002-R02-00.pdf)

661 Marshall, J. R. (1962). The morphology of the upper Solway salt marshes. *Scottish Geographical*
662 *Magazine*, 78(2), 81–99. <https://doi.org/10.1080/00369226208735859>

663 Odd, N. V. M., & Murphy, D. G. (1992). *Particulate pollutants in the North Sea: Calibration of a*
664 *20 km gridded 3D model simulating a representative annual cycle of mud transport* (Report SR
665 292). Wallingford: HR Wallingford.

666 Phelan, N., Shaw, A., & Baylis, A. (2011). The extent of saltmarsh in England and Wales: 2006-
667 2009. Bristol: Environment Agency. Retrieved from
668 [https://www.gov.uk/government/publications/the-extent-of-saltmarsh-in-england-and-wales-](https://www.gov.uk/government/publications/the-extent-of-saltmarsh-in-england-and-wales-2006-to-2009)
669 [2006-to-2009](https://www.gov.uk/government/publications/the-extent-of-saltmarsh-in-england-and-wales-2006-to-2009)

670 Prandle, D., Lane, A., & Manning, A. J. (2005). Estuaries are not so unique. *Geophysical*
671 *Research Letters*, 32(23). <https://doi.org/10.1029/2005gl024797>

- Pringle, A. W. (1995). Erosion of a cyclic saltmarsh in Morecambe Bay, north-west England. *Earth Surface Processes and Landforms*, 20(5), 387–405. <https://doi.org/10.1002/esp.3290200502>
- Spearman, J., Baugh, J., Feates, N., Dearnaley, M., & Eccles, D. (2014). Small estuary, big port – progress in the management of the Stour-Orwell estuary system. *Estuarine, Coastal and Shelf Science*, 150, 299–311. <https://doi.org/10.1016/j.ecss.2014.07.003>
- Wernette, P., Shortridge, A., Lusch, D. P., & Arbogast, A. F. (2017). Accounting for positional uncertainty in historical shoreline change analysis without ground reference information. *International Journal of Remote Sensing*, 38(13), 3906–3922. <https://doi.org/10.1080/01431161.2017.1303218>
- Wolters, M., Garbutt, A., & Bakker, J. P. (2005). Salt-marsh restoration: Evaluating the success of de-embankments in north-west Europe. *Biological Conservation*, 123(2), 249–268. <https://doi.org/10.1016/j.biocon.2004.11.013>
- Yapp, R. H., Johns, D., & Jones, O. T. (1917). The Salt Marshes of the Dovey Estuary. *The Journal of Ecology*, 5(2), 65. <https://doi.org/10.2307/2255644>
- Zuur, A. F., Ieno, E. N., Walker, N., Saveliev, A. A., & Smith, G. M. (2009). Mixed effects models and extensions in ecology with R. New York: Springer NY. <https://doi.org/10.1007/978-0-387-87458-6>

Table 1. Rates of lateral and vertical marsh change per region. Mean \pm S.E values per region for marsh lateral expansion rates, and the rate of marsh vertical accretion, minus the rate of relative sea level rise, to give the ‘accretion balance’. Measures of vertical marsh accretion rates were unavailable for the Morecambe region.

Region	Lateral expansion (ha yr ⁻¹)	Accretion balance (mm yr ⁻¹)
Solway	0.88 \pm 1.17	15.41 \pm 14.53 (Marshall, 1962)
Morecambe	2.94 \pm 0.37	n.a.
Cardigan	2.31 \pm 1.37	8.25 \pm 4.06 (Kestner, 1975)
Wash	1.27 \pm 0.00	46.17 \pm 26.87 (Shi, 1993)
Essex-Kent	-6.42 \pm 3.55	3.20 \pm 3.56 (Cundy & Croudace, 1996)
Solent	-3.59 \pm 1.65	2.91 \pm 0.84 (van der Wal & Pye, 2004)

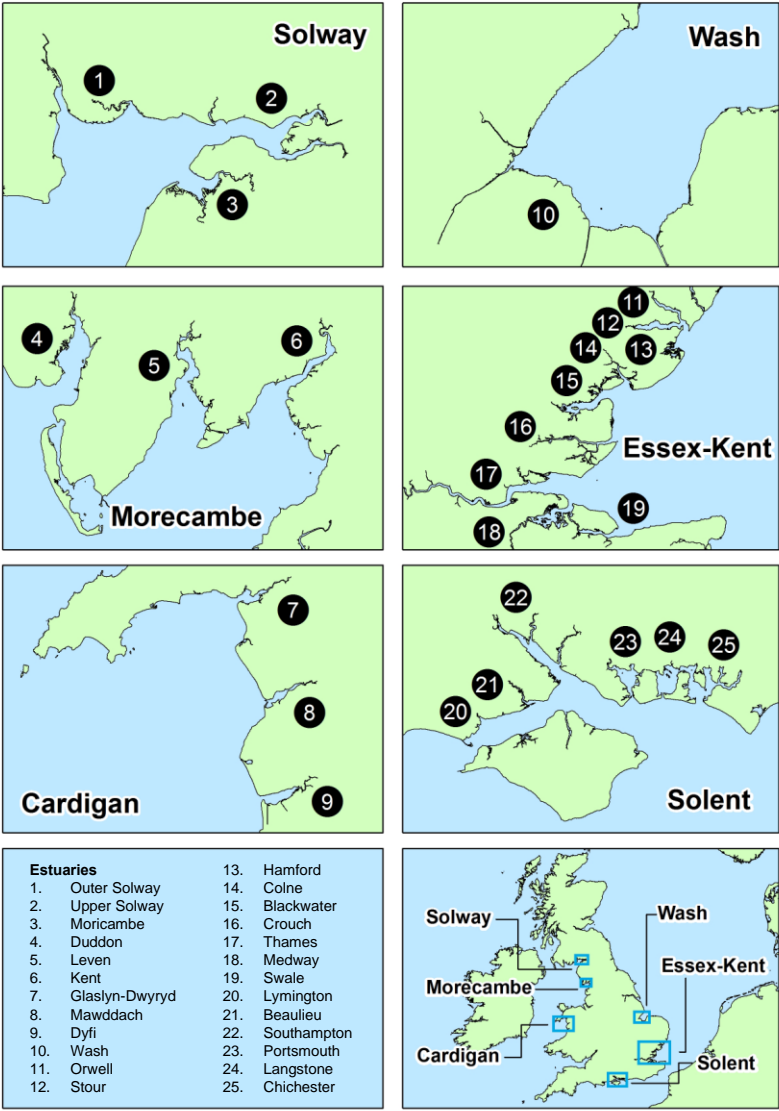


Figure 1. Estuaries examined within each region. A total of 25 estuaries separated into 6 regions across Great Britain.

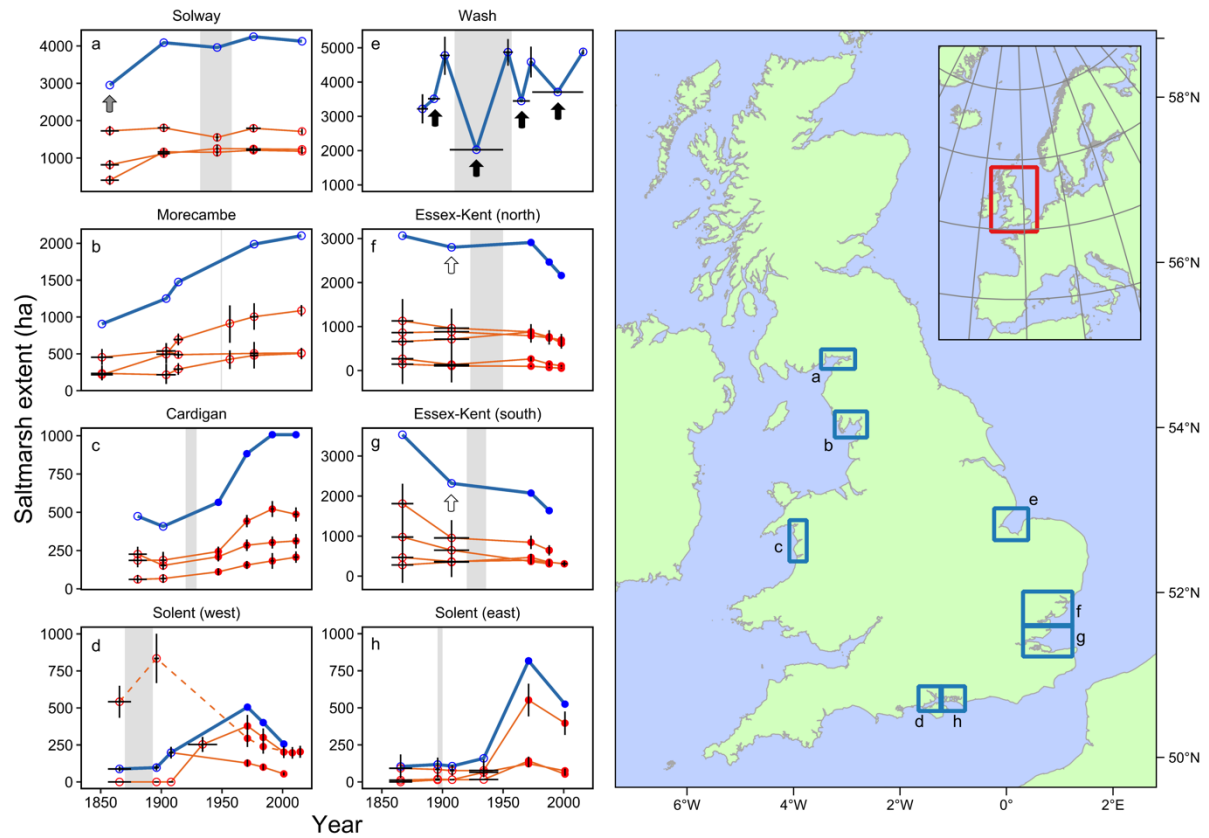


Figure 2. Change in estuarine-scale marsh extent across Great Britain. Regional- (blue line) and estuarine-scale (orange line) change in areal extent of salt marshes between 1856 and 2016 from photographs (filled circles) or maps (hollow circles). Arrows indicate occurrences of embankment (solid arrow), canalisation (grey arrow) or collapse of sea walls after storms (hollow arrow). Grey shading indicates *Spartina spp.* Colonisation in each region. Vertical error bars indicate 95% confidence intervals in marsh area extent. Horizontal lines indicate the dates over which surveys of marsh extent were carried out. Essex-Kent and Solent regions have been subdivided for ease of presentation. Regional-scale marsh change (blue line) only includes marsh extent measures for all estuary in a given region and year. Marsh change in Southampton estuary (panel d: dashed line) was excluded from the regional-scale marsh change line due to paucity of contiguous cover in saltmarsh extent across multiple years.

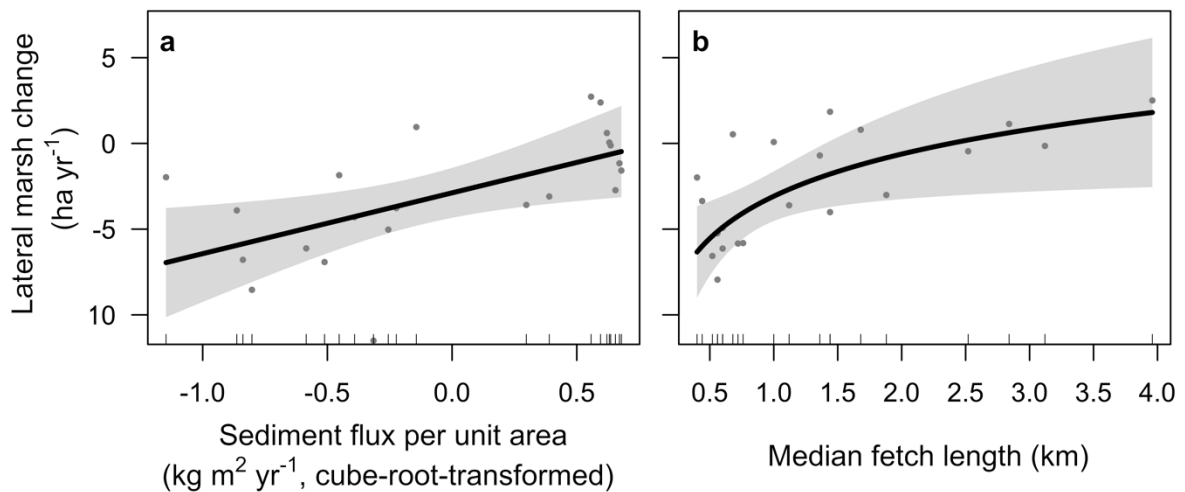


Figure 3. Relationships of estuarine-scale lateral marsh change with two significant predictor variables identified from a best-fit linear regression model on data for 1967 to 2016 ($n = 22$): **a** sediment flux per unit area and **b** median fetch length. Data points represent distribution of standardised partial residuals. Solid lines represent model-fit through the data, bounded by 95% confidence intervals (solid grey shading). Tick marks along the bottom of each plot denote deciles of the distribution of each predictor value.

724

725

Geophysical Research Letters

726

Supporting Information for

727

Sediment supply explains long-term and large-scale patterns in saltmarsh lateral expansion and erosion

728

729

Cai J. T. Ladd^{1,2}, Mollie F. Duggan-Edwards¹, Tjeerd J. Bouma³, Jordi F. Pagès⁴, Martin W. Skov¹

730

¹School of Ocean Sciences, Bangor University, Menai Bridge, LL59 5AB, UK.

731

²Department of Geography, Swansea University, Swansea, SA2 8PP, UK.

732

³Department of Estuarine and Delta Systems, Royal Netherlands Institute for Sea Research (NIOZ), Utrecht University, 4400

733

AC Yerseke, P.O. Box 140, The Netherlands.

734

⁴Centre d'Estudis Avançats de Blanes (CEAB-CSIC), Blanes, 17300, Catalonia (Spain).

735

736

737

738

Contents of this file

739

740

Tables S1 to S3

741

Text S1 to S3

742

743

744

Introduction

745

The following supporting information contains details on how error resulting from digitising saltmarsh extent across Great Britain was calculated (Text S1), how net sediment fluxes values across marsh complexes were calculated and validated from the unvegetated/vegetated ratio (Text S2), and a report on the full statistical treatment applied to our data (Text S3). Tables S1 to S3 provide further details on literature that corroborates marsh extent change detected from the GIS study, the variables used to explain change in marsh extent, and the results of a Stepwise Linear Regression model used to identify which key variables explain marsh change respectively.

746

747

748

749

750

751

752

753

Region	Area of rapid change	Description and reference
Solway	Rapid expansion and erosion phases of all major marshes in each estuary	OS maps record the expansion and erosion of these larger marshes throughout the Solway region, with a net increase in marsh extent. A study by Marshall (1962) reaches a similar conclusion from interpreting maps (1856-1864) and aerial photographs (1946). Marshall (1962) also investigated aspects of saltmarsh morphology (accretion rates, areas of erosion and expansion and channel configuration) to corroborate their findings and conclude that there is close agreement between phases of expansion and erosion observed in the field and change recorded from maps. Rapid expansion of Caerlaverock is also described by Bridson (1980) from maps dating back to 1654, in agreement with Marshall (1962). Firth et al. (2000) and CCO (2011) describe the rapid expansion and erosion of different parts of Rockcliffe marsh (Inner Solway) and the marshes in Moricambe Bay since 1776 and 1864 from literature searches and site visits, which we observe in the OS maps.
Morecambe	Rapid erosion and expansion phases in all estuaries	OS maps record the overall expansion of marshes throughout the Morecambe Bay region, with individual marshes undergoing extensive erosion and accretion phases. Of the most drastic change, phases of erosion in Silverdale marsh have been documented by Pringle (1995) from repeat transect measurements between 1983 and 1992, which is out of phase with marsh expansion at Grange-over-Sands on the opposite side of the estuary, described in field surveys by Gray (1972). All estuaries in Morecambe Bay region are considered dynamic and have experienced rapid changes in saltmarsh extent determined from site visits, historical records and modelling data (CH2M HILL, 2013a, 2013b, 2013c; Dixon-Gough, 2006). These observations support marsh change observed in OS maps.
Cardigan	Rapid expansion of marshes in the outer estuary	OS maps reveal that marshes throughout the Cardigan Bay region have expanded gradually, with more rapid rates of expansion around the 1950s. Field sketches made by Yapp (1917) include detailed vegetation surveys of the Dyfi estuary in the mid 1910s which show a similar extent of saltmarshes to the OS maps. Rapid expansion of the marshes in the outer estuary in the late 1940s is documented by Chater & Jones (1957) from site surveys. Both studies are in agreement with observations of marsh change from OS maps.
Wash	Rapid expansion following reclamation	OS maps document the step-wise loss of marshlands to reclamation, followed by phases of new marsh growth in front of seawalls throughout the Wash embayment. Kestner (1962) reconstructed past area cover of salt marsh extent for the Wash by knowing the dates when seawalls were constructed. Kestner (1975) later described the mechanism by which sediment deposits in front of the sea wall, allowing marshes to rapidly colonise and expand. These phases of reclamation and new marsh growth are in agreement with marsh change determined from OS maps.
Essex-Kent	Gradual erosion across all estuaries, with some areas of rapid marsh expansion	OS maps record the gradual erosion of marshes across Essex-Kent, with small areas of rapid expansion or erosion subject to embankment/deembankment. Burd (1992) report in detail the numerous areas of embankment and deembankment from history books, parish and estate records, property deeds, maps and historical surveys from the 17 th century onwards. Areas of reclaimed and deembanked marshland is reported by Wolters et al. (2005). Burd (1992) also report that the government at the time were aware of marsh erosion and more frequent flooding due to land subsidence and rising sea levels. Kirby (2013) and Spearman et al. (2014) also document marsh decline from historical maps and illustrations in the northern and southern parts of the region respectively.
Solent	Rapid expansion across all estuaries	OS maps record the expansion of marshes across the Solent region. Baily & Inkpen (2013) account for the rapid expansion because of the colonisation and spread of the pioneer-marsh hybrid <i>Spartina townsendii</i> , and later, fertile allotetraploid species <i>Spartina anglica</i> , onto tidal flats across the region. Baily & Inkpen (2013) support this argument by referring to a number of articles published during this period that document the nature and spread of <i>Spartina spp.</i> across the region. Baily & Inkpen (2013) did find issues with the accuracy of maps compared to aerial photographs, however much of the error was due to not knowing the date a map was surveyed (only when it was published) when comparing to an aerial photograph, and revision errors where marshes were copied over to successive map editions thus not representing the true marsh extent of that year. Both error terms were accounted for in our study and described in Text S1.

Table S1. Literature searched to determine whether marsh change from maps can be considered ‘real’.

	Lateral expansion (ha yr ⁻¹)	Vertical accretion (mm yr ⁻¹) ± S.D.	Relative sea level rise (mm yr ⁻¹)	Net sediment flux (kg m ⁻² yr ⁻¹) (2006-2009)	Suspended sediment conc. (mg l ⁻¹) (2000)
Solway	(1970-2016)	(1961)	(1960-2015)		
Outer Solway	0.14	21.43 ± 10.56	2.28 ± 0.65	0.313	404.22
Upper Solway	2.22	11.79 ± 18.12	2.28 ± 0.65	0.302	404.22
Moricambe	0.27	25.40 ± 0.00	2.28 ± 0.65	0.281	404.22
Morecambe	(1967-2010)		(1960-2015)		
Duddon	2.84	NA	2.34 ± 0.68	0.211	291.49
Leven	3.35	NA	2.34 ± 0.68	0.173	313.42
Kent	2.62	NA	2.34 ± 0.68	0.251	313.42
Cardigan	(1969-2013)		(1938-2016)		
Glaslyn-Dwryrd	1.56	NA	2.27 ± 0.30	0.212	89.37
Mawddach	1.48	NA	2.27 ± 0.30	0.155	NA
Dyfi	3.89	10.29 ± 4.06 (1988-1989)	2.27 ± 0.30	0.239	111.03
Wash	(1972-2016)		(1955-2016)		
Wash	1.27	48.00 ± 26.87 (1956-1962)	1.83 ± 0.38	0.257	295.97
Essex-Kent	(1973-1998)		(1933-2016)		
Orwell	-1.85	NA	1.89 ± 0.27	-0.003	64.46
Stour	-6.39	NA	1.89 ± 0.27	-0.017	64.46
Hamford	-9.98	NA	1.89 ± 0.27	-0.517	59.51
Colne	-3.81	NA	1.89 ± 0.27	0.059	78.69
Blackwater	-7.99	4.84 ± 5.00 (1963-1998)	1.22 ± 0.19	-0.200	122.68
Crouch	-6.50	6.70 ± 0.00 (1897-1994)	1.22 ± 0.19	-0.011	106.40
Thames	-3.93	3.93 ± 1.38 (1963-1998)	1.22 ± 0.19	-0.060	NA
Medway	-13.22	4.05 ± 2.05 (1989)	1.22 ± 0.19	-0.031	86.05
Swale	-4.11	NA	1.22 ± 0.19	0.026	NA
Solent	(1971-2001)		(1961-2016)		
Lymington	-4.86	5.2 ± 0.00 (1893-1995)	1.62 ± 0.46	-0.134	42.54
Beaulieu	-2.44	3.3 ± 0.00 (1893-1995)	1.62 ± 0.46	-0.224	54.12
Southampton	-4.31	4.8 ± 0.14 (1870-1995)	1.62 ± 0.46	-0.093	102.87
Portsmouth	-2.72	NA	1.62 ± 0.46	-1.509	83.39
Langstone	-1.45	1.5 ± 0.00 (1907-1995)	1.62 ± 0.46	-0.643	79.57
Chichester	-5.77	NA	1.62 ± 0.46	-0.590	78.56

Table S2. Site characteristics for all 25 estuaries divided into 6 regions. Parentheses indicate the timescales over which rates were measured, or in which empirical data was used to derive values. These dates are representative of either the entire Great Britain, a whole region, or a specific estuary.

	Bedload sediment flux (m ³ yr ⁻¹)	Wind storm frequency (n yr ⁻¹)	River flood frequency (n yr ⁻¹)	Median fetch length (m)	Tidal range (m)
				(2006-2009)	(2006-2009)
Solway	(2010)	(1961-2008)			
Outer Solway	10,000,000	0.02	1.34 (1979-2014)	3,120	5.92
Upper Solway	100,000	0.02	-1.36 (1963-2014)	2,520	5.92
Moricambe	0	0.02	0.00	1,880	5.92
Morecambe	(2010)	(1957-2015)			
Duddon	10,000	0.01	0.79 (1968-2014)	1,000	6.12
Leven	1,000,000	-0.15	0.44 (1939-2014)	1,440	6.36
Kent	10,000,000	-0.15	0.28 (1968-2014)	3,960	6.36
Cardigan	(2010)	(1957-2015)			
Glaslyn-Dwryrd	NA	0.09	0.34 (1961-2014)	520	3.04
Mawddach	NA	0.09	NA	1,040	2.94
Dyfi	-1,000,000	0.09	0.02 (1962-2013)	1,360	2.90
Wash	(2002)	(1969-2015)			
Wash	10,000,000	-0.01	0.04 (1939-1996)	2,840	4.42
Essex-Kent	(2002)	(1957-2015)			
Orwell	10,000	0.04	0.11 (1964-1996)	400	2.64
Stour	10,000	0.04	-0.13 (1928-1992)	600	2.64
Hamford	1,000	0.04	0.00	560	2.64
Colne	10,000	0.04	0.07 (1959-2014)	720	3.24
Blackwater	10,000	0.04	0.10 (1932-1968)	520	3.48
Crouch	1,000,000	-0.50	0.21 (1976-2014)	560	3.76
Thames	-1,000,000	-0.50	0.27 (1883-2014)	600	5.00
Medway	100,000	-0.13	-0.02 (1956-2014)	600	4.08
Swale	10,000	-0.13	0.00	760	3.90
Solent	(1998)	(1957-2015)			
Lymington	0	0.06	0.57 (1960-2014)	1,440	1.56
Beaulieu	0	0.06	NA	240	2.26
Southampton	10,000	0.06	0.05 (1972-2014)	440	2.72
Portsmouth	1,000	0.06	0.26 (1951-2014)	680	2.82
Langstone	1,000	0.06	0.11 (1979-2014)	1,680	2.98
Chichester	1,000	0.06	0.04 (1967-2014)	1,120	2.98

Table S2. *Continued.*

Model variables	Estimate	SE	t-Value	P value	R ²
Best model fit (AIC = 116.79, F = 9.95, df = 3, 18, P < 0.001***, R ² = 0.62)					
Net sediment flux (kg m ⁻² yr ⁻¹)	3.547	1.332	2.662	0.016*	0.48
Median fetch length (km)	3.549	1.323	2.682	0.015*	0.46
Bedload sediment flux (m ³ yr ⁻¹)	-0.014	0.010	-1.495	0.152 n.s.	0.06

P < 0.05*, P < 0.01**, P < 0.001***, n.s. = P > 0.05.

Table S3. Predictor variables explaining lateral saltmarsh change (1967-2016) identified by best fit models (Stepwise Linear Regression) for 25 estuaries across Great Britain.

Text S1. Estimating error in saltmarsh area cover.

We calculated change in the areal extent of salt marshes across Great Britain using maps and aerial photographs. Analysis was done in ArcGIS 10.1. In order to quantify an error term associated with these measurements, we calculated the Root Mean Squared Error (RMSE) which describes the average deviation of observed points from their true positions (Wernette et al., 2017). Four independent RMSE sources are associated with geographical data: displacement of the basemap, to which historical maps and aerial photographs are referenced, from its 'true' location on the Earth's surface (RMSE_B); distortions in historical maps and aerial photographs that introduce error when georeferencing to a basemap (RMSE_G); interpreter error when digitising the salt marsh at a given scale (RMSE_I), and; errors introduced by the cartographer when presenting spatial data on a map (not relevant for aerial photographs) (RMSE_M). Because each error source is independent, they can be added for a total error estimate. To determine distances, in metres, below which 95% of the positional errors in delineated salt marsh edges are expected to fall, FGDC (1998) recommend the added RMSE values are multiplied by 1.7308 in order to calculate RMSE₉₅, given as:

$$RMSE_{95} = 1.7308 \left(\sqrt{RMSE_B^2 + RMSE_G^2 + RMSE_I^2 + RMSE_M^2} \right)$$

Maps produced between 1842 and 1952 (Six-inch County Series Edition) the Ordnance Survey (OS), the national mapping agency of the UK, were produced using ground surveys. Demarcating the seaward limit of the salt marsh accurately is dependent on the cartographer's capacity to survey difficult-to-reach or dangerous areas, and distinguish the edge of the marsh which is often 'fuzzy' (due to patchy growth of plants) (Baily & Collier, 2010; Baily, 2011; Baily & Inkpen, 2013). OS standards on the quality and accuracy of saltmarsh surveying were not stringent (Baily & Inkpen, 2013) therefore the marsh edge is sometimes represented as a stamped symbol without a clearly defined margin (Baily & Inkpen, 2013). OS maps produced after 1952 (National Series Edition maps) were compiled using a combination of ground surveys and aerial photographs. Delineating the marsh edge from aerial photographs accurately depends on surveyor capacity to correctly distinguish plants from other features (such as macroalgae patches) as well as the quality of the aerial image. There is no specific guidance set by the OS on demarcating the marsh edge from aerial photographs (OS, pers. comm., 2018). Baily and Inkpen (2013) assessed how successful OS ground-surveys were at determining the marsh edge by comparing maps with aerial photographs captured near the map publication date. Where maps were surveyed at similar times to when images were taken, both media were in close agreement.

A value for the positional error of digitised marsh edge (map or photo) from the true position (RMSE_I) was not given by Baily and Inkpen (2013). To calculate RMSE_I, we selected an example marsh boundary (a 5 km section saltmarsh edge in the Wash) to digitise at very high resolution (vertices placed every metre) at high magnification to capture the 'true' marsh edge from an OS map.

Resolution of the map was then scaled to 1:7500, and the marsh edge was digitised once again to capture the 'interpreted' marsh edge. Distance from the 'interpreted' line to the 'true' line was calculated every 20 metres along perpendicular lines from the 'true' line. This is the same procedure used when assessing interpreter error for maps and aerial photographs. $RMSE_I$ is given as:

$$RMSE_I = \sqrt{\left(\frac{\sum d^2}{n}\right)}$$

Where:

d is the distance between the 'true' and 'interpreted' marsh edge
 n is the number of distance measurements.

An additional error term, associated with maps produced from ground surveys only, is the interpretation of the surveyor of where the marsh edge lies which is then reproduced on a map as a line or stamp ($RMSE_M$). Given that marsh edges from maps and photos have been shown to be in close agreement (Baily & Inkpen, 2013), $RMSE_M$ is assumed to be of the same magnitude as $RMSE_I$:

$$RMSE_M = RMSE_I$$

Both $RMSE_M$ and $RMSE_I$ should be included for estimates of marsh extent taken from maps that have drawn from ground surveys.

$RMSE_G$ in maps and aerial photographs can arise during and after the survey. For maps, inaccuracies arise when noting positions from traditional trigonometry surveys or modern Geographical Positioning Systems. After publication, historical maps can distort over time through shrinkage and stretching before digitisation occurred. For aerial photographs, tilt, pitch and yaw of the aeroplane will affect the angle at which images were taken. Unevenness of the topography being captured will also cause distortions to the image. After acquisition, both the original film and reprints can distort over time once produced. These issues reduce the accuracy of features on maps and aerial photographs once images are georeferenced. Georeferencing distortion can be calculated by the distance from which the source deviates from a reference position (Jongepier et al., 2016) as follows:

$$RMSE_G = \sqrt{\left(\frac{\sum V_{xy}^2}{n - 2}\right)}$$

Where n is the number of points and V_{xy} is a displacement vector made up of vector distances v_x and v_y (in metres) between the distorted points and the reference positions. Both V_x and V_y are calculated as follows:

$$V_{xy} = \sqrt{(v_x^2 + v_y^2)}$$

$RMSE_G$ was calculated for all maps and photographs to OS 1:2500 basemaps as reference, using MapAnalyst (Jenny & Hurni, 2011). 12 well-distributed control points were identified in both the source and OS 1:2500 maps and the $RMSE_G$ between them was calculated using a Helmert transformation (Jongepier et al., 2016). Measurements of marsh extent for the Essex-Kent and Solent regions were taken from Cooper et al. (2001) and Baily & Pearson (2007). Cooper et al. (2001) does not report $RMSE_G$ for their survey, however Baily and Pearson (2007) report a precision value

of between ± 3 and 5 m. An average $RMSE_G$ of 4 metres was taken for their survey and applied to Essex-Kent and Cardigan Bay regions where aerial photography was used to delineate marsh extent.

The OS 1:2500 maps used as a reference for measuring distortions in older maps and aerial photographs in this study are themselves subject to some positional error between the 'real life' position and that recorded on the map known as $RMSE_B$. For the OS 1:2500, $RMSE_B$ of 1.1 metres has been calculated (HMLR, 2016). $RMSE_{95}$ is a linear measure (units in metres). In order to express $RMSE_{95}$ for areal measures, we constructed a buffer area around the inner and outer circumference of each marsh where the width was $RMSE_{95}$ calculated for each source (Wernette et al., 2017). The buffer area indicates the minimum and maximum size of the marsh to provide an error term for each extent measurement, representing a 95% confidence interval. Calculating a buffer area was not possible for values taken from Cooper et al. (2001) and Baily and Pearson (2007), and no error term is reported by these authors. A marsh buffer area was therefore estimated for each study. The buffer area was estimated by resampling marsh extent from aerial photographs of Cardigan Bay, but at the image scales used by Cooper et al. (2001) and Baily and Pearson (2007) (1:5,000 and 1:10,000 respectively). $RMSE_{95}$ was recalculated, then the percentage difference in area extent between delineated marsh extent and maximum/minimum area buffers were calculated for each scale. Marsh extent was found to vary by ± 18.4 and $\pm 20.0\%$ at scales of 1:5,000 and 1:10,000 respectively. These error margins were applied to the values of marsh extent taken from Cooper et al. (2001) and Baily and Pearson (2007) as the $RMSE_{95}$ error term. The final error term for marsh area extent can be considered conservative, because accuracy in delineating the marsh edge in many cases will be much higher. For example, where the back of the marsh is bounded by a clearly-defined seawall that can be mapped to a high degree of accuracy.

After the OS produced first edition maps (County and National Series), revisions were soon needed to keep maps up-to-date in a rapidly developing landscape. However, revisions did not always include complete re-surveys of an area. Revisions tended to be made only for areas heavily used by people, whilst less important features were simply copied over from the previous edition known as 'partial-revisions' (Baily & Inkpen, 2013). Salt marshes were not always resurveyed during map revisions, and when revisions occurred, the specific area that had been revised was not always recorded (Baily, 2011). In our study, revision error was accounted for by comparing map revisions against first editions of each marsh in each estuary. On the assumption that the marsh boundary is likely to change during a ~ 30 year period, marshes that had near-identical boundaries in both first and revised editions were considered copied, so areal extent was not calculated.

All $RMSE$ values are contained within the attributes table of the marsh extent change GIS layer accessible via the Environmental Information Data Centre repository (DOI: 10.5285/03b62fd0-41e2-4355-9a06-1697117f0717).

Text S2. Calculating and validating net sediment flux.

Sediment supply is a key predictor of long-term marsh stability (e.g. Kirwan et al., 2016), yet empirical measurements of sediment flux across marshes are sparse (Ganju et al., 2015). Recent work has shown that the ratio of unvegetated surfaces such as tidal channels, salt pans and marsh edges (sites of sediment erosion) to vegetated marsh areas (sites of sediment accretion) can act as a proxy for external sediment supply (Ganju et al., 2017). We calculated the UVVR values for all marshes in our study and used regression fits from (Ganju et al., 2017) to derive measures of net sediment flux. We also validated the flux rates against estimated measures of suspended sediment concentration for UK estuaries.

We used a combined Great Britain-wide saltmarsh extent shapefile (collated by the UK Environment Agency [EA] and the Scottish National Heritage [SNH]) to calculate the UVVR for each estuary. Both the EA and SNH shapefiles represent the vegetated portions of marshes across Great Britain and distinguish vegetated marshes from tidal channels and salt pans. The EA captured colour aerial images with 10 cm resolution for the UK coastline between 2006 and 2009. Images were georeferenced with root mean square error ranging from 10 cm to 1 m. Marsh delineation was done manually, and digitally using various feature-identification techniques. Creeks less than 1.5 m wide and marshes less than 5m² were overlooked. In cases where there was low confidence in mapping results, site visits were made to ground-truth the digitised marsh surface (Phelan et al., 2011). The SNH mapped salt marshes larger than 3 ha from colour aerial photographs captured between 2003 and 2009 at a 1:4,000 scale across the Scottish coastline. All creeks, salt pans, and other marsh features were mapped when above the mapping resolution. Marsh edges were compared to field surveys to ensure accuracy (Haynes, 2016).

In a GIS, we used both saltmarsh extent shapefiles to calculate the area of vegetated portions for each marsh complex within our target estuary. We then applied a workflow of ArcGIS 10.1 tools to outline the overall marsh complex, thereby effectively separating tidal channel and salt pan features from the vegetated marsh surface. The original shapefile was then subtracted from this 'boundary' layer to calculate the area of unvegetated portions within the marsh complex (e.g. Figure S1). UVVR was then calculated (A_{UV}/A_V) for all 25 estuaries. We then regressed the values of UVVR and net sediment flux reported in Ganju et al. (2017) to give us an equation for predicting net sediment flux ($y = -0.855 \ln x + 0.330$). We fitted the values of UVVR calculated for each marsh complex in our study into the regression equation to derive measures of net sediment flux.

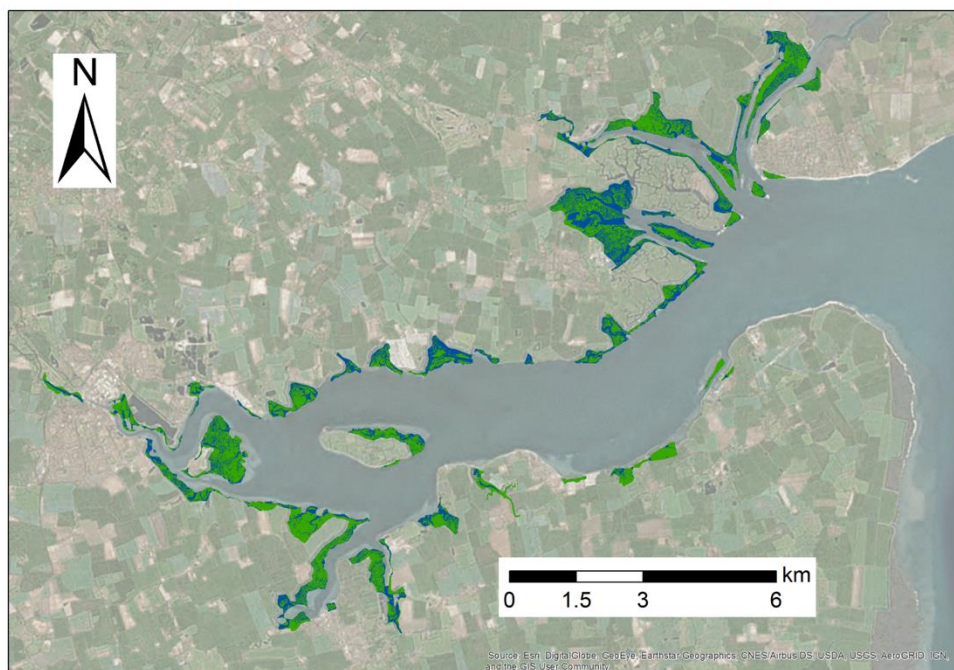


Figure S1. Example of how vegetated and unvegetated portions of a marsh are identified for the Blackwater estuary, south-east Great Britain. Unvegetated areas are shown in blue, vegetated surfaces are shown in green. Saltmarsh extent was taken from the UK Environment Agency, and the marsh boundary was determined using a series of polygon processing tools in ArcGIS 10.1. Imagery from the ArcGIS World Imagery Basemap.

To validate our use of sediment flux estimated from UVVR as a predictor of lateral marsh change, we correlated sediment flux values against an estimated measure of estuarine maximum static time- and depth-averaged fine cohesive suspended sediment concentration (SSC_E) (Manning & Whitehouse, 2012). SSC_E is indicative of sediment supply, and has been shown to broadly represent real conditions in validation studies (Prandle et al., 2005, see Figure 4). We used a Pearson correlation to find that SSC and sediment flux were significantly positively correlated ($R = 0.68$, $p < 0.001$) (Figure S2). We therefore consider our use of net sediment flux a suitable indicator of external sediment supply. SSC_E values for each estuary are shown in Table S2.

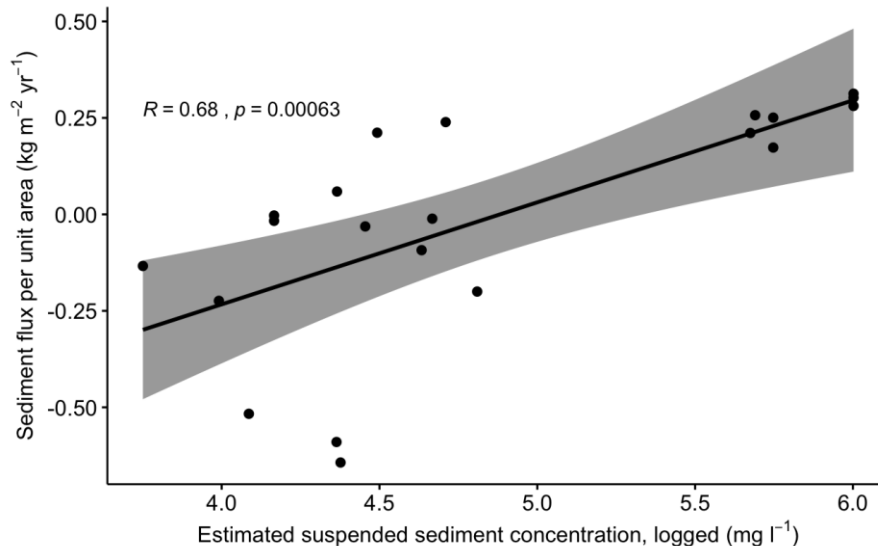


Figure S2. Pearson correlation between sediment flux and estimated suspended sediment concentration ($R = 0.68$, $p < 0.001$).

Text S3. Data analysis and model selection.

In this section, we present the statistical analysis used to determine which environmental drivers best describe rate of saltmarsh change across Great Britain. All statistical analyses are carried out using the 'R' software package. The data used in the statistical analysis is accessible via the Environmental Information Data Centre repository (DOI: 10.5285/03b62fd0-41e2-4355-9a06-1697117f0717).

Prior to selecting a statistical model, we tested the necessary assumptions of each statistical model. We begin by loading the dataset, graphics package `ggplot2`, and some additional functions held in the `additional_functions.R` file:

```
library(ggplot2)
source("/Users/Home/Code/additional_functions.R")
marshes<-read.csv("/Users/Home/Data/PredictorVariables.csv",header=T)
```

There are 4 cases in the dataset where data on river flood frequency change and bedload sediment flux were unavailable of a given estuary. We therefore subset the dataset by removing NAs:

```
marshes_RM<-marshes[complete.cases(marshes),]
```

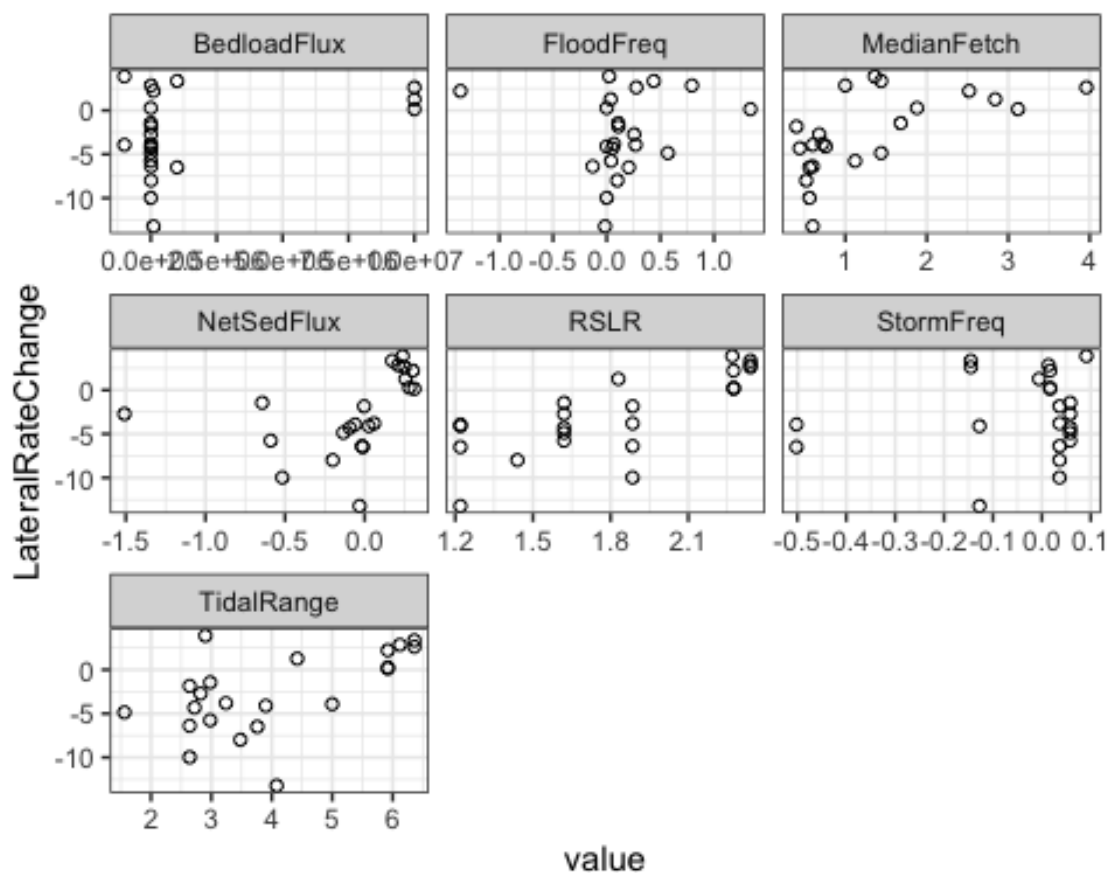
Using the subset dataset without NAs (`marshes_RM`), we begin our data exploration by investigating how each predictor variable relates to rate of saltmarsh change. To

make this easier, we create a new object containing the response and predictor variables only:

```
library(dplyr)
library(tidyr)

marshcheck<-marshes_RM[-c(1:3)]

marshcheck %>%
  gather(-LateralRateChange, key="var", value="value") %>%
  ggplot(aes(x=value, y=LateralRateChange))+
  geom_point(shape=1)+
  facet_wrap(~var, scales="free_x")+
  theme_bw()
```



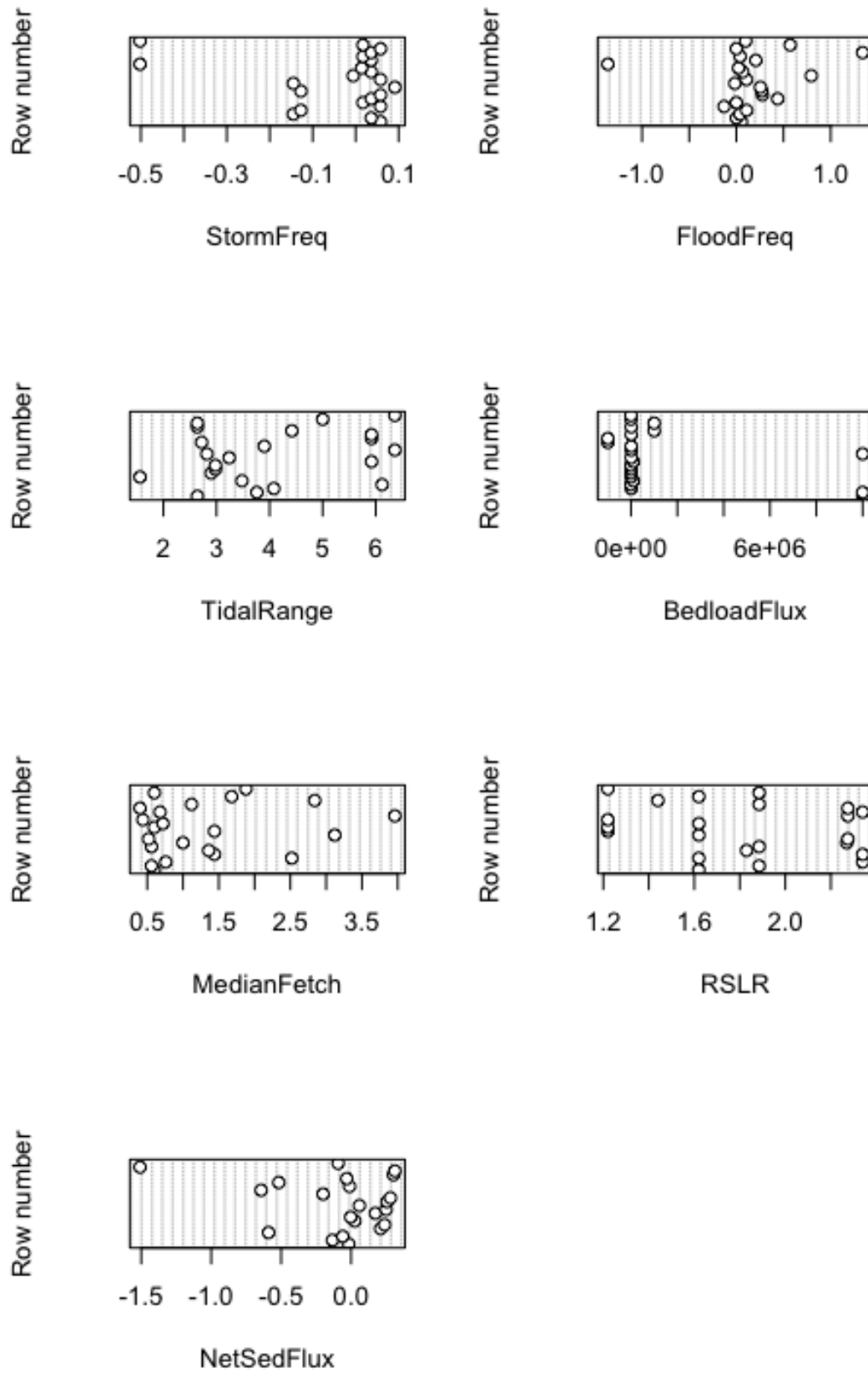
It appears that increases in fetch distance, sediment flux per unit area in/out of the marsh, relative sea level rise rate, and tidal range, may all be associated with shifts from marsh erosion to expansion. The other predictor variables do not appear to have a relationship with lateral marsh change. We used Cleveland dotplots to identify any extreme outliers in our dataset. Outliers may have a significant impact on the results. The data is organised along the y-axis only by row name (i.e. the order in which it was entered into the dataframe):

```
par(mfrow=c(2,2))

lapply(X=c("StormFreq", "FloodFreq", "TidalRange", "BedloadFlux", "MedianFetch
```



```
987 ", "RSLR", "NetSedFlux"), FUN=function(s)  
988   dotchart(sample(marshcheck[, s]), xlab=s, ylab="Row number"))
```



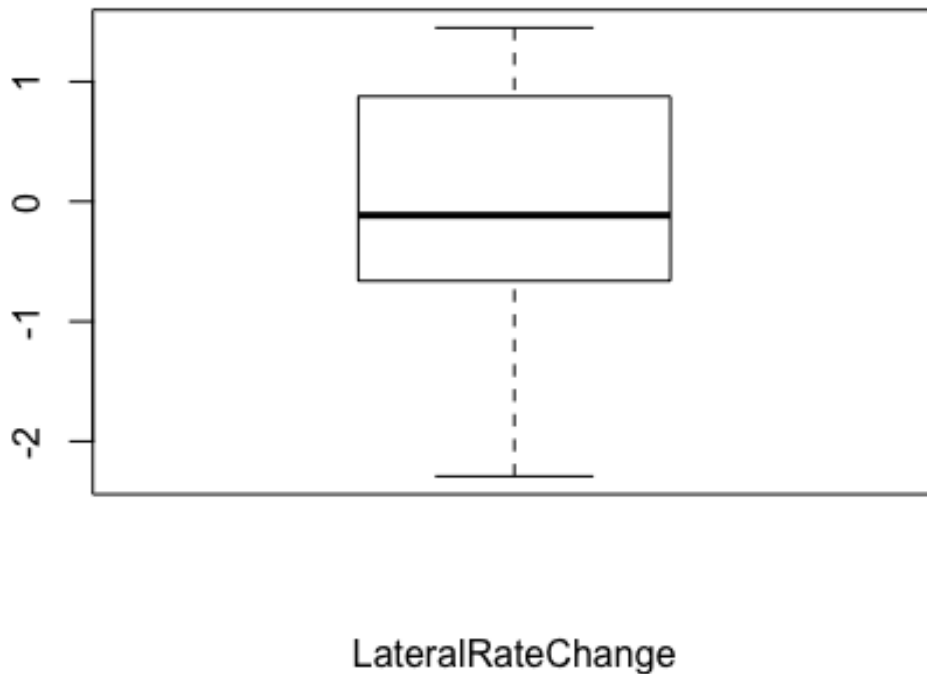
989

990

Large variation from the centre of data clusters suggests the presence of outliers. *StormFreq*, *FloodFreq*, *BedLoadFlux*, and *NetSedFlux* however none appears to be unprecedented. These are not unprecedented amounts, but may affect our model results. We will consider their effect when testing the final model assumptions.

To check whether the response variable has a normal distribution, we build a boxplot, and scale the y axis to make their ranges comparable:

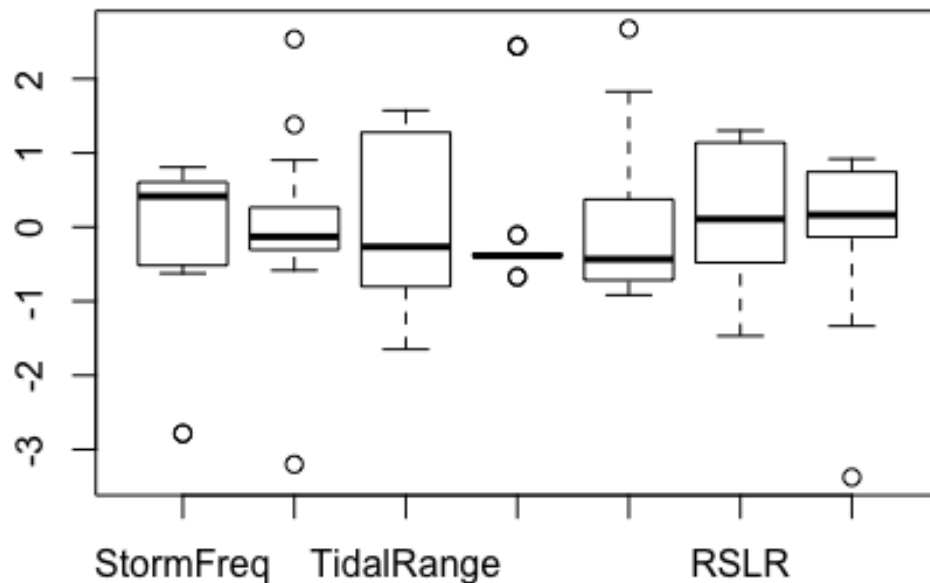
```
boxplot(scale(marshes_RM$LateralRateChange),
        xlab="LateralRateChange")
```



```
shapiro.test(marshes_RM$LateralRateChange)
##
##  Shapiro-Wilk normality test
##
## data:  marshes_RM$LateralRateChange
## W = 0.96174, p-value = 0.5253
```

There is no evidence of skew. We next consider the distribution of all predictor variables:

```
boxplot(scale(marshes_RM[, 5:11]))
```



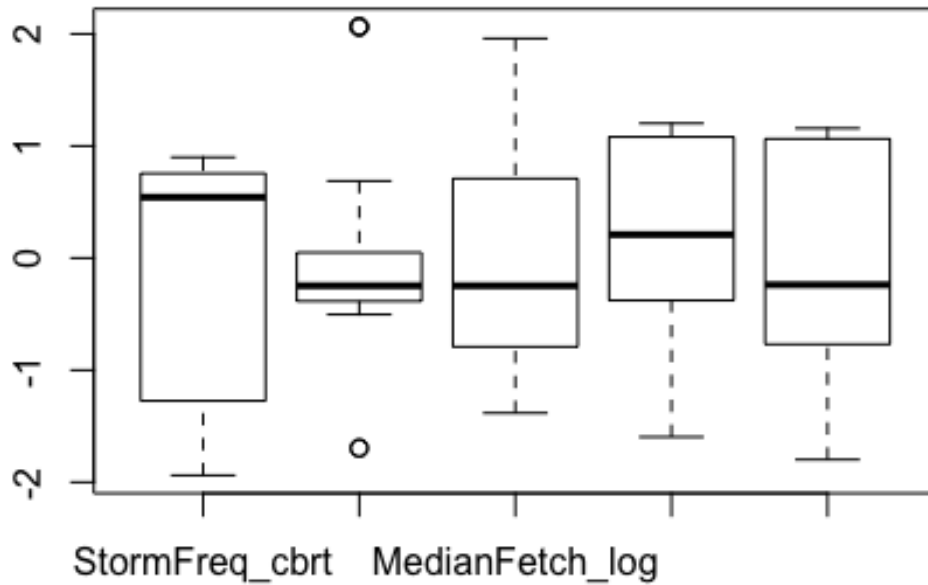
1010

1011 There is some evidence of skew in the predictor variables, notably for *StormFreq*,
 1012 *BedLoadFlux*, *MedianFetch*, and *RSLR*. Some of these are likely influenced by
 1013 outliers in the data. Transformations using log- and cube-root- (capable of
 1014 transforming both negative and positive values. See the *Math.cbirt* function in the
 1015 *additional_functions.R* file) may produce more normal populations suitable for
 1016 parametric modelling. We apply the transformations and add these to our
 1017 dataframe:

```
1018 marshes_RM$StormFreq_cbirt<-Math.cbirt(marshes_RM$StormFreq)
1019 marshes_RM$BedloadFlux_cbirt<-Math.cbirt(marshes_RM$BedloadFlux)
1020 marshes_RM$MedianFetch_log<-log(marshes_RM$MedianFetch)
1021 marshes_RM$RSLR_log<-log(marshes_RM$RSLR)
1022 marshes_RM$NetSedFlux_cbirt<-Math.cbirt(marshes_RM$NetSedFlux)
```

1023 We next inspect the distribution of the transformed predictor variables:

```
1024 boxplot(scale(marshes_RM[, 12:16]))
```



1025

1026

The transformed predictor variables now have a more symmetric distribution. We consider the distribution of our data suitable for parametric modelling.

1027

1028

Prior to using a parametric model to determine which suite of variables best explains rate of saltmarsh areal extent change, we need to check for high collinearity

1029

1030

between predictor variables, and reduce it if necessary. We can examine the

1031

Variance Inflation Factor associated with each predictor variable (see `corvif`

1032

function in `additional_functions.R` file) to assess how much variance of an

1033

estimated regression coefficient increases if variables are correlated. Values over 3

1034

are a cause for concern (Zuur et al., 2009):

1035

```
corvif(marshes_RM[,c("StormFreq_cbirt", "FloodFreq", "TidalRange", "BedloadFlux_cbirt", "MedianFetch_log", "RSLR_log", "NetSedFlux_cbirt")])
```

1036

1037

```
## Correlations of the variables
```

1038

```
##
```

1039

```
##           StormFreq_cbirt  FloodFreq  TidalRange  BedloadFlux_cbirt
```

1040

```
## StormFreq_cbirt      1.00000000 -0.06642290 -0.4471729  -0.2730783
```

1041

```
## FloodFreq            -0.06642290  1.00000000  0.1015293   0.2630995
```

1042

```
## TidalRange           -0.44717292  0.10152926  1.00000000   0.4555946
```

1043

```
## BedloadFlux_cbirt   -0.27307833  0.26309947  0.4555946   1.00000000
```

1044

```
## MedianFetch_log     -0.01892536  0.07428223  0.5719886   0.5589768
```

1045

```
## RSLR_log             0.41207815  0.06286752  0.4446737   0.2756686
```

1046

```
## NetSedFlux_cbirt    -0.21050716  0.02345964  0.7079982   0.4041456
```

1047

```
##           MedianFetch_log  RSLR_log  NetSedFlux_cbirt
```

1048

```
## StormFreq_cbirt      -0.01892536  0.41207815  -0.21050716
```

1049

```
## FloodFreq            0.07428223  0.06286752   0.02345964
```

1050

```
## TidalRange           0.57198855  0.44467372   0.70799815
```

```

1051 ## BedloadFlux_cbrt      0.55897675 0.27566864      0.40414564
1052 ## MedianFetch_log       1.00000000 0.59019663      0.58825538
1053 ## RSLR_log              0.59019663 1.00000000      0.60255965
1054 ## NetSedFlux_cbrt      0.58825538 0.60255965      1.00000000
1055 ##
1056 ##
1057 ## Variance inflation factors

1058 ## Warning in summary.lm(object): essentially perfect fit: summary may be
1059 ## unreliable

```

```

1060 ##                               GVIF
1061 ## StormFreq_cbrt      3.519783
1062 ## FloodFreq           1.099187
1063 ## TidalRange          3.490519
1064 ## BedloadFlux_cbrt   1.751466
1065 ## MedianFetch_log     2.334006
1066 ## RSLR_log            4.365753
1067 ## NetSedFlux_cbrt    2.883363

```

1068 There is high collinearity caused by *RSLR_Log* (VIF = 4.37). We test whether
1069 collinearity has dropped to acceptable levels after excluding *RSLR_Log*:

```

1070 corvif(marshes_RM[,c("StormFreq_cbrt", "FloodFreq", "TidalRange", "BedloadFlu
1071 x_cbrt", "MedianFetch_log", "NetSedFlux_cbrt")])

```

```

1072 ## Correlations of the variables
1073 ##
1074 ##           StormFreq_cbrt   FloodFreq   TidalRange   BedloadFlux_cbrt
1075 ## StormFreq_cbrt      1.00000000 -0.06642290 -0.4471729      -0.2730783
1076 ## FloodFreq          -0.06642290  1.00000000  0.1015293       0.2630995
1077 ## TidalRange         -0.44717292  0.10152926  1.0000000       0.4555946
1078 ## BedloadFlux_cbrt   -0.27307833  0.26309947  0.4555946       1.0000000
1079 ## MedianFetch_log    -0.01892536  0.07428223  0.5719886       0.5589768
1080 ## NetSedFlux_cbrt   -0.21050716  0.02345964  0.7079982       0.4041456
1081 ##           MedianFetch_log   NetSedFlux_cbrt
1082 ## StormFreq_cbrt      -0.01892536      -0.21050716
1083 ## FloodFreq           0.07428223       0.02345964
1084 ## TidalRange          0.57198855       0.70799815
1085 ## BedloadFlux_cbrt    0.55897675       0.40414564
1086 ## MedianFetch_log     1.00000000       0.58825538
1087 ## NetSedFlux_cbrt     0.58825538       1.00000000
1088 ##
1089 ##
1090 ## Variance inflation factors

```

```

1091 ## Warning in summary.lm(object): essentially perfect fit: summary may be
1092 ## unreliable

```

```

1093 ##                               GVIF
1094 ## StormFreq_cbrt      1.502641
1095 ## FloodFreq           1.093159
1096 ## TidalRange          2.869967
1097 ## BedloadFlux_cbrt   1.739354
1098 ## MedianFetch_log     2.257387
1099 ## NetSedFlux_cbrt    2.257476

```

All VIF scores are below 3, so we therefore proceed with investigating which predictor variables best explain lateral marsh change using General Linear Models (GLMs). Before proceeding with model selection, we need to account for any spatial autocorrelation that might invalidate our model. We use hierarchical clustering to identify groups in our data.

Accounting for spatial autocorrelation can dramatically improve model performance, and help to avoid biased estimates of Type I error. We will examine whether there are groupings between our estuaries, based on their pairwise Euclidean distances. If so, this will form a random factor in the model structure.

We start by creating the matrix of Euclidean distances between estuaries:

```
library(gmt)

distance_estuary_matrix=matrix(NA,length(marshes_RM$Estuary),length(marshes_RM$Estuary))
for(est1 in 1:length(marshes_RM$Estuary)){
  for(est2 in est1:length(marshes_RM$Estuary)){

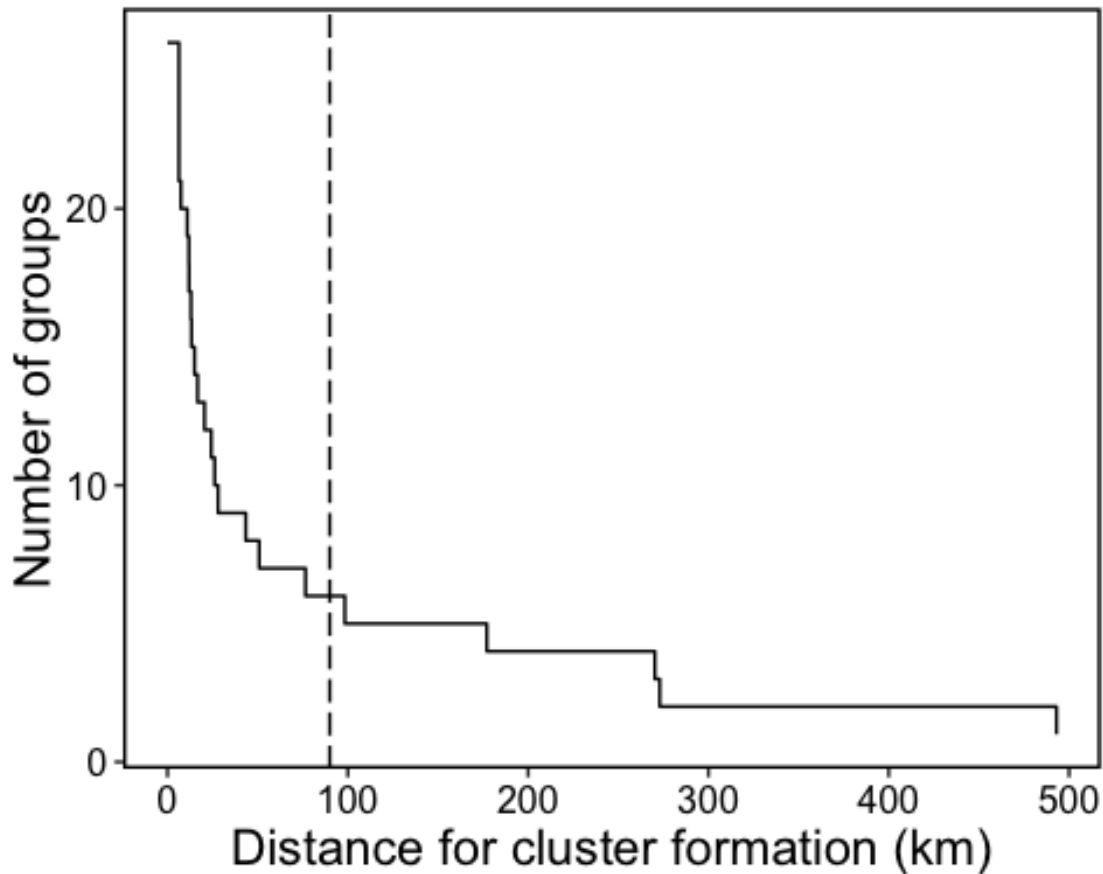
    distance_estuary_matrix[est1,est2]=geodist(marshes_RM$Latitude[est1],marshes_RM$Longitude[est1],
    marshes_RM$Latitude[est2],marshes_RM$Longitude[est2], units="km")
  }}
distance_estuary_matrix=as.dist(t(distance_estuary_matrix))
full=hclust(distance_estuary_matrix,method="complete")
```

We can extract the cophenetic distance between groups to select a value for the inflection point in intra-estuary group variance and use Elbow plots to validate our selection. First, we prepare our data:

```
dist_clust<-data.frame(data.frame(unique(as.numeric(cophenetic(full))))[order((unique(as.numeric(cophenetic(full)))),decreasing=T),)])
names(dist_clust)<-"distance"
dist_clust$group<-seq.int(nrow(dist_clust))
add_zero<-c(0,26)
dist_clust<-rbind(dist_clust,add_zero)
```

Now we can plot the number of groups against distance to form the clusters:

```
ggplot(dist_clust,aes(distance,group))+
  geom_step()+
  geom_vline(xintercept=90,linetype="longdash")+
  xlab("Distance for cluster formation (km)") +
  ylab("Number of groups")
```



1138

1139

1140

1141

1142

Number of groups reduces exponentially with distance, and we see an ‘evening out’ at around 90 km, suggesting this is a suitable inflection point to distinguish our groups. This ends up producing 6 distinct hierarchical clusters. We validate our selection of 6 clusters using Elbow plots with k-means clustering method:

1143

1144

1145

1146

1147

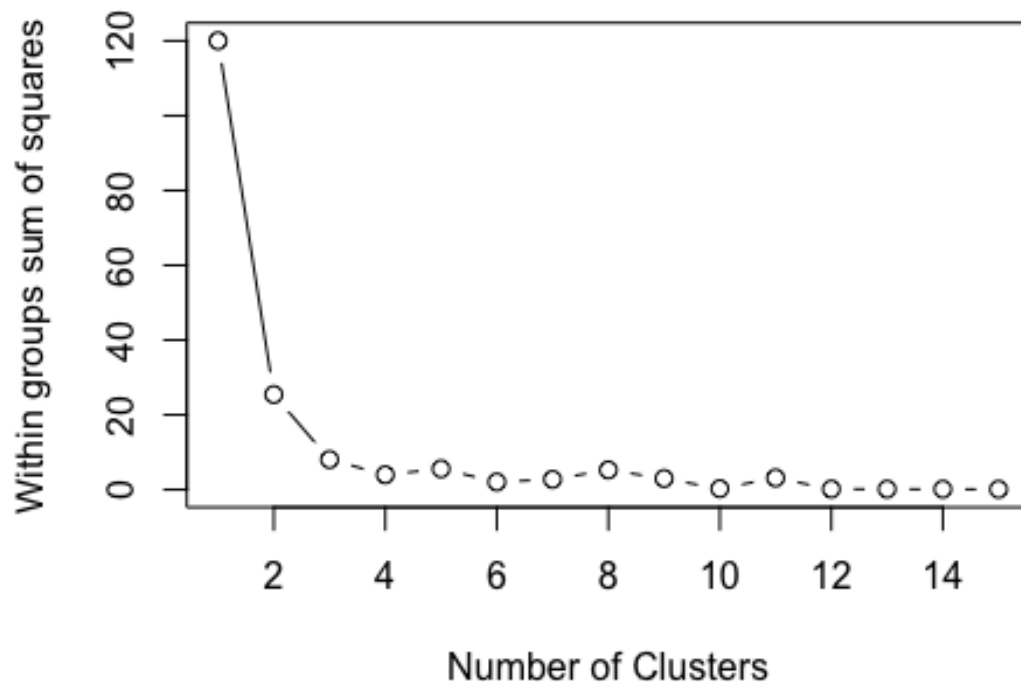
1148

1149

1150

```
wss<-(nrow(subset(marshes_RM,select=c(Longitude,Latitude)))-1)*sum(apply(s
subset(marshes_RM,select=c(Longitude,Latitude)),2,var))
for (i in 2:15) wss[i] <- sum(kmeans(subset(marshes_RM,select=c(Longitude,
Latitude)),
                           centers=i)$withinss)

plot(1:15, wss, type="b", xlab="Number of Clusters",
      ylab="Within groups sum of squares")
```



1151

1152

Sum of squares within groups flattens out at 6 groups. This is in agreement with the previous plot, so we can justify grouping our estuaries into 6 hierarchical clusters.

1153

1154

We now cut the hierarchical clustering analysis tree at the 90 inflection point to form our 6 groups and bind as a new column to our dataframe:

1155

1156

```
group=cutree(full, h=90)
marshes_RM=cbind(marshes_RM,group) # column bind the dataset and the previously determined grouping
marshes_RM$group<-as.factor(marshes_RM$group)
```

1157

1158

1159

1160

If we inspect the dataframe marshes, we see that group identity is the same as the region in which each estuary occurs. We will now build a linear model and determine whether inclusion of region as a random factor improves the model.

1161

1162

1163

Before selecting an appropriate GLM, we consider whether inclusion of location (represented by *group* from the hierarchical clustering analysis) as a random effect term significantly improves a maximal model fit using a Restricted Maximum

1164

1165

1166

Likelihood (REML) approach (Zuur et al., 2009).

1167

We construct two models, one with a random effect, and one without. Anova tables can be used to see if there is a significant difference between the models. Since the model is using REML, we need to adapt the significance level using the L Ratio (Zuur et al., 2009):

1168

1169

1170

1171

```
library(nlme)
m1<-gls(LateralRateChange
~ 1 + StormFreq_cbrt+FloodFreq+TidalRange+BedloadFlux_cbrt+MedianF
```

1172

1173

1174

```

1175 etch_log+NetSedFlux_cbrt,
1176     method = "REML",
1177     control="optim",
1178     data=marshes_RM)
1179
1180 m2<-lme(LateralRateChange
1181     ~ 1 + StormFreq_cbrt+FloodFreq+TidalRange+BedloadFlux_cbrt+MedianF
1182 etch_log+NetSedFlux_cbrt,
1183     random = ~1|group,
1184     method = "REML",
1185     control="optim",
1186     data=marshes_RM)
1187
1188 anova(m1,m2)

```

	##	Model	df	AIC	BIC	logLik	Test	L.Ratio	p-value
1189	##	m1	1	8	117.1529	122.8173	-50.57646		
1190	##	m2	2	9	117.3425	123.7150	-49.67127	1 vs 2	1.810397 0.1785

```

1191
1192 0.5*(1-pchisq(1.810397,1))
1193
1194 ## [1] 0.08923031

```

Though close ($p=0.089$), there is no significant difference between the models. We can therefore use the more parsimonious model (*m1*, without accounting for spatial groups).

Stepwise Linear Regression can be used to identify which suite of predictor variables best explain the response variable, based on whichever models produce the lowest AIC scores. We apply a Stepwise Linear Regression to our data, using a forwards-and-backwards selection criterion to drop terms based on AIC scores. We switch from *gls* to *lm* to do this:

```

1202 m3<-lm(LateralRateChange
1203     ~ StormFreq_cbrt+FloodFreq+TidalRange+BedloadFlux_cbrt+MedianFetch_
1204 log+NetSedFlux_cbrt,
1205     data=marshes_RM)
1206
1207 step(m3,direction="both")

```

	##	Start:	AIC=56.25
1208	##	LateralRateChange ~ StormFreq_cbrt + FloodFreq + TidalRange +	
1209	##	BedloadFlux_cbrt + MedianFetch_log + NetSedFlux_cbrt	
1210	##		
1211	##		
1212	##		
1213	##	- FloodFreq	1 4.115 154.22 54.842
1214	##	- TidalRange	1 4.605 154.71 54.911
1215	##	- StormFreq_cbrt	1 9.586 159.69 55.609
1216	##	<none>	150.11 56.247
1217	##	- BedloadFlux_cbrt	1 16.489 166.59 56.539
1218	##	- NetSedFlux_cbrt	1 37.316 187.42 59.131
1219	##	- MedianFetch_log	1 39.266 189.37 59.359
1220	##		
1221	##	Step:	AIC=54.84
1222	##	LateralRateChange ~ StormFreq_cbrt + TidalRange + BedloadFlux_cbrt +	

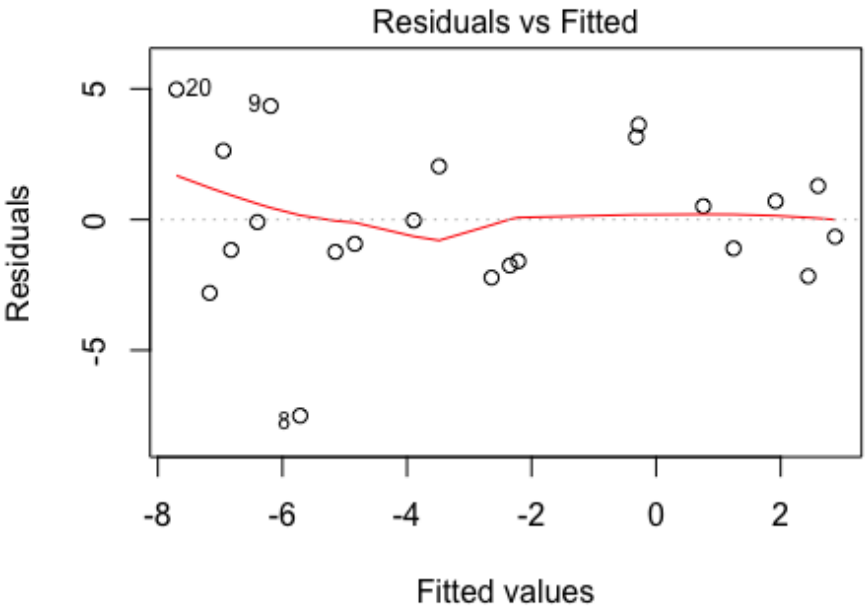

```

1223 ##      MedianFetch_log + NetSedFlux_cbrt
1224 ##
1225 ##              Df Sum of Sq      RSS      AIC
1226 ## - TidalRange      1      5.309 159.53 53.586
1227 ## - StormFreq_cbrt    1     10.152 164.37 54.244
1228 ## - BedloadFlux_cbrt  1     13.370 167.59 54.671
1229 ## <none>                        154.22 54.842
1230 ## + FloodFreq        1      4.115 150.11 56.247
1231 ## - NetSedFlux_cbrt   1     35.490 189.71 57.398
1232 ## - MedianFetch_log   1     37.604 191.82 57.642
1233 ##
1234 ## Step: AIC=53.59
1235 ## LateralRateChange ~ StormFreq_cbrt + BedloadFlux_cbrt + MedianFetch_log
1236 +
1237 ##      NetSedFlux_cbrt
1238 ##
1239 ##              Df Sum of Sq      RSS      AIC
1240 ## - StormFreq_cbrt    1      5.686 165.22 52.357
1241 ## - BedloadFlux_cbrt  1     12.994 172.52 53.309
1242 ## <none>                        159.53 53.586
1243 ## + TidalRange        1      5.309 154.22 54.842
1244 ## + FloodFreq          1      4.820 154.71 54.911
1245 ## - MedianFetch_log    1     52.575 212.10 57.853
1246 ## - NetSedFlux_cbrt    1     70.467 230.00 59.635
1247 ##
1248 ## Step: AIC=52.36
1249 ## LateralRateChange ~ BedloadFlux_cbrt + MedianFetch_log + NetSedFlux_cbr
1250 t
1251 ##
1252 ##              Df Sum of Sq      RSS      AIC
1253 ## <none>                        165.22 52.357
1254 ## - BedloadFlux_cbrt    1     20.510 185.73 52.931
1255 ## + StormFreq_cbrt      1      5.686 159.53 53.586
1256 ## + FloodFreq           1      4.912 160.30 53.693
1257 ## + TidalRange          1      0.843 164.37 54.244
1258 ## - NetSedFlux_cbrt     1     65.049 230.26 57.660
1259 ## - MedianFetch_log     1     66.010 231.23 57.752
1260 ##
1261 ## Call:
1262 ## lm(formula = LateralRateChange ~ BedloadFlux_cbrt + MedianFetch_log +
1263 ##      NetSedFlux_cbrt, data = marshes_RM)
1264 ##
1265 ## Coefficients:
1266 ##      (Intercept)  BedloadFlux_cbrt  MedianFetch_log  NetSedFlux_cbrt
1267 ##      -2.12177      -0.01429           3.54861           3.54688
1268
1269 The predictor variables that should be retained in the minimal adequate model are
1270 BedLoadFlux_cbrt, MedianFetch_log, and NetSedFlux_cbrt. We assign the
1271 predictor variables to a minimal adequate model:
1272
1273 m4<-lm(LateralRateChange
1274 ~ BedloadFlux_cbrt+log(MedianFetch)+NetSedFlux_cbrt,
1275 data=marshes_RM)

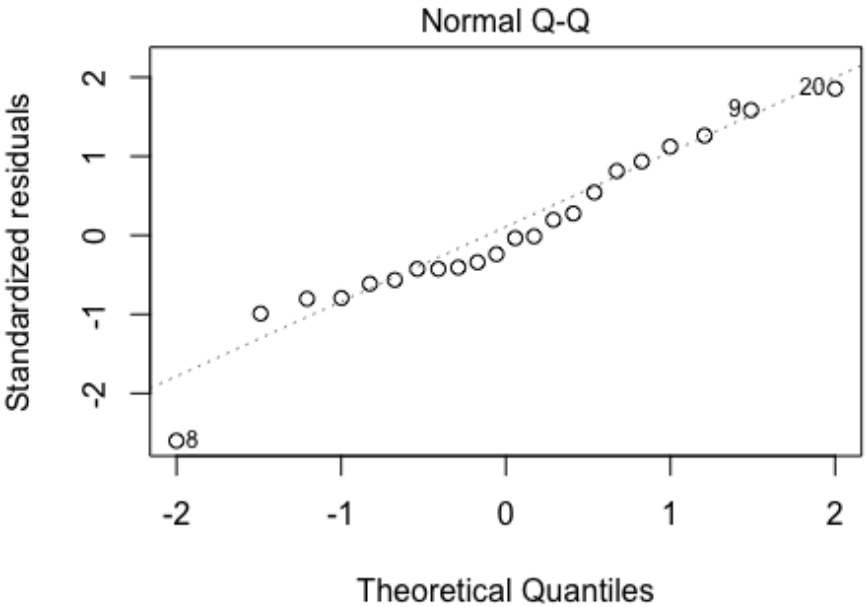
```

We check for heteroscedacity and bias in the model residuals, to check whether assumption of Heterogeneity of Variance have been violated:

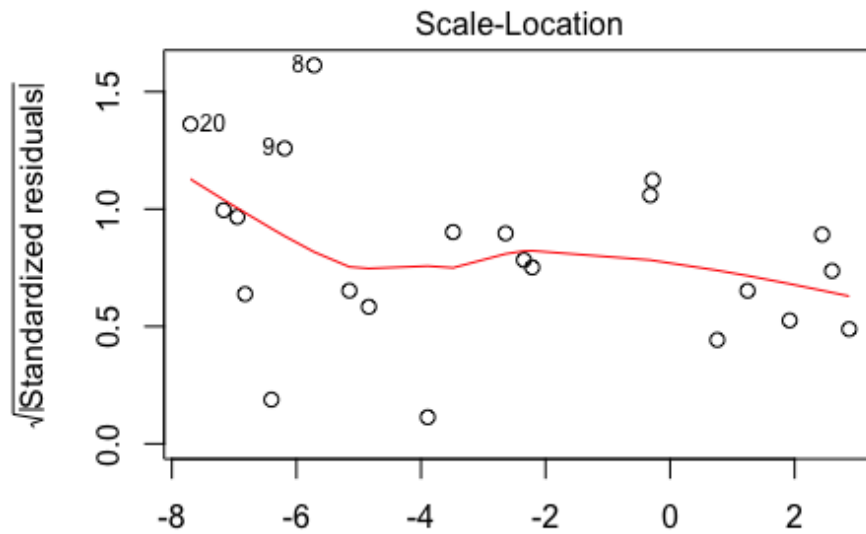
`plot(m4)`



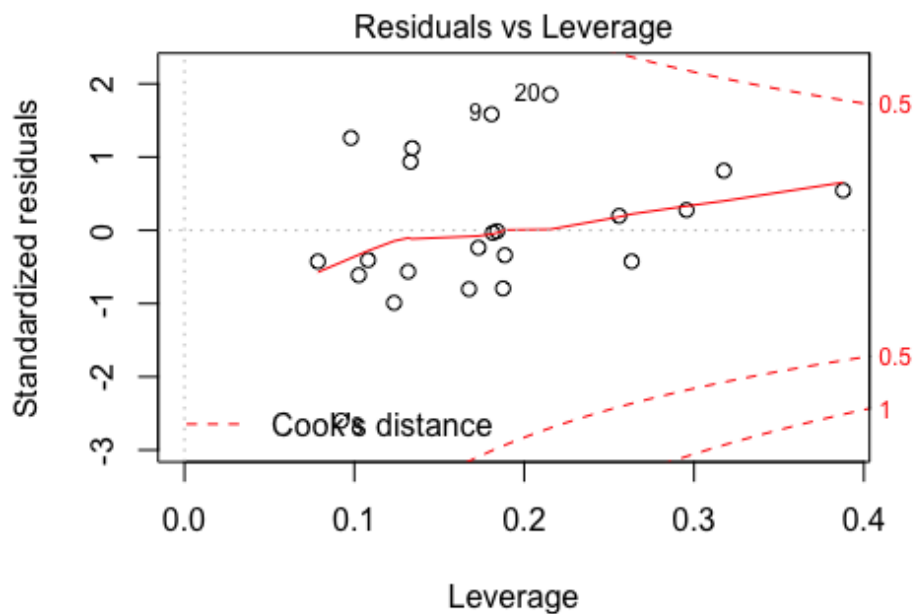
`teralRateChange ~ BedloadFlux_cbrt + log(MedianFetch) + NetSed`



`teralRateChange ~ BedloadFlux_cbrt + log(MedianFetch) + NetSed`



teralRateChange ~ BedloadFlux_cbrt + log(MedianFetch) + NetSed



teralRateChange ~ BedloadFlux_cbrt + log(MedianFetch) + NetSed

There are no major issues with the model assumptions. We can now report the model results. We use anova tables to identify significant factors in our model using 'Type I' sums of squares, and consider which terms of the model are significant, the AIC score, and use the *relaimpo* package to calculate relative importance for the linear model using R^2 partitioned by averaging over orders:

```
library(relaimpo)
anova(m4)
```

```

1288 ## Analysis of Variance Table
1289 ##
1290 ## Response: LateralRateChange
1291 ##           Df Sum Sq Mean Sq F value    Pr(>F)
1292 ## BedloadFlux_cbrt  1  22.987   22.987   2.5044 0.1309427
1293 ## log(MedianFetch)  1 185.898  185.898  20.2533 0.0002768 ***
1294 ## NetSedFlux_cbrt   1  65.049   65.049   7.0870 0.0158758 *
1295 ## Residuals       18 165.216    9.179
1296 ## ---
1297 ## Signif. codes:  0 '***' 0.001 '**' 0.01 '*' 0.05 '.' 0.1 ' ' 1

1298 summary(m4)

1299 ##
1300 ## Call:
1301 ## lm(formula = LateralRateChange ~ BedloadFlux_cbrt + log(MedianFetch) +
1302 ##     NetSedFlux_cbrt, data = marshes_RM)
1303 ##
1304 ## Residuals:
1305 ##      Min       1Q   Median       3Q      Max
1306 ## -7.5047 -1.5047 -0.3771  1.8486  4.9780
1307 ##
1308 ## Coefficients:
1309 ##              Estimate Std. Error t value Pr(>|t|)
1310 ## (Intercept)   -2.121770    0.758995  -2.795   0.0120 *
1311 ## BedloadFlux_cbrt -0.014293    0.009561  -1.495   0.1523
1312 ## log(MedianFetch)  3.548614    1.323257   2.682   0.0152 *
1313 ## NetSedFlux_cbrt  3.546880    1.332338   2.662   0.0159 *
1314 ## ---
1315 ## Signif. codes:  0 '***' 0.001 '**' 0.01 '*' 0.05 '.' 0.1 ' ' 1
1316 ##
1317 ## Residual standard error: 3.03 on 18 degrees of freedom
1318 ## Multiple R-squared:  0.6238, Adjusted R-squared:  0.5611
1319 ## F-statistic: 9.948 on 3 and 18 DF,  p-value: 0.0004326

1320 AIC(m4)

1321 ## [1] 116.7899

1322 calc.relimp(m4,type=c("lmg"),rela=T)

1323 ## Response variable: LateralRateChange
1324 ## Total response variance: 20.91194
1325 ## Analysis based on 22 observations
1326 ##
1327 ## 3 Regressors:
1328 ## BedloadFlux_cbrt log(MedianFetch) NetSedFlux_cbrt
1329 ## Proportion of variance explained by model: 62.38%
1330 ## Metrics are normalized to sum to 100% (rela=TRUE).
1331 ##
1332 ## Relative importance metrics:
1333 ##
1334 ##              lmg
1335 ## BedloadFlux_cbrt 0.06176616
1336 ## log(MedianFetch) 0.45986451

```

```

1337 ## NetSedFlux_cbrt 0.47836933
1338 ##
1339 ## Average coefficients for different model sizes:
1340 ##
1341 ##           1X           2Xs           3Xs
1342 ## BedloadFlux_cbrt 0.01246703 -0.007295296 -0.01429271
1343 ## log(MedianFetch) 4.44960924 3.960577731 3.54861396
1344 ## NetSedFlux_cbrt 5.08045110 4.288503610 3.54687976

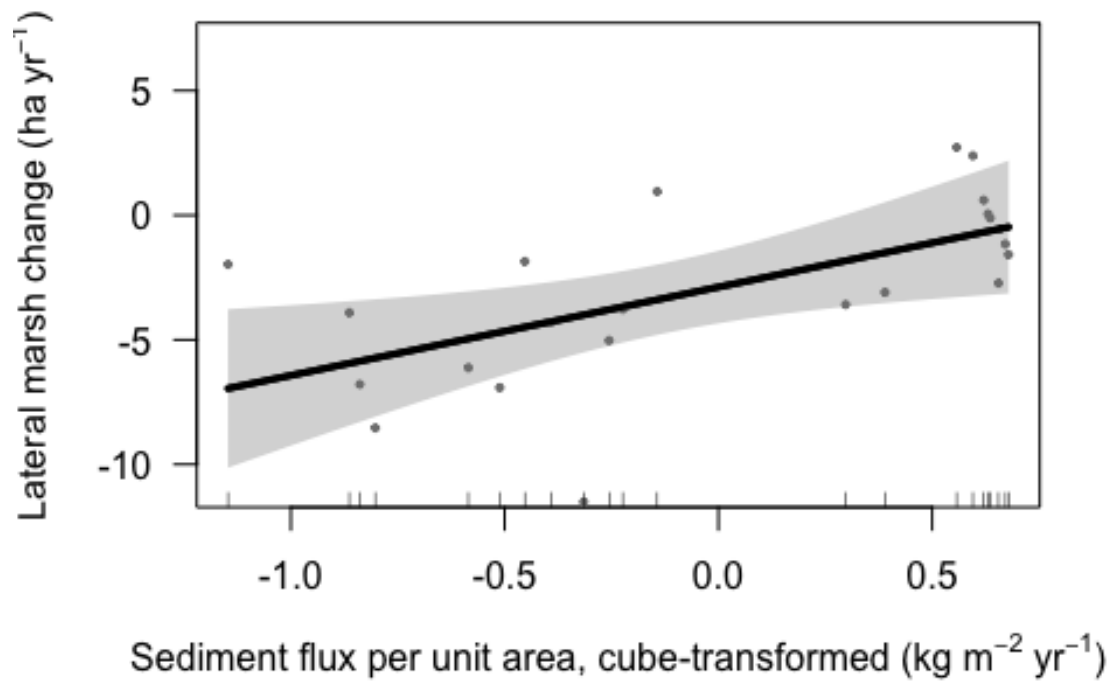
```

1345 *MedianFetch_Log* and *NetSedFlux_cbrt* are both significant terms, whereas
 1346 *BedloadFlux_cbrt* is not. The AIC score of the minimal adequate model is 116.79.
 1347 The proportion of variance explained by the model is 62.38%, and of that variance,
 1348 *MedianFetch_log* and *NetSedFlux_cbrt* account for nearly half each (46% and 48%
 1349 respectively). Finally, visualise the significant terms of the regression model using the
 1350 *visreg* package. Marshes shift from a trend of expansion to erosion in response to
 1351 increased fetch length and sediment supply:

```

1352 library(visreg)
1353
1354 visreg(m4,"NetSedFlux_cbrt",
1355       ylim=c(-11,7),
1356       scale="response",
1357       partial=T,
1358       rug=T,
1359       line=list(col="black"),
1360       xlab=expression("Sediment flux per unit area, cube-transformed (kg
1361 m^-2 yr^-1)"),
1362       ylab=expression("Lateral marsh change (ha yr^-1)"))

```

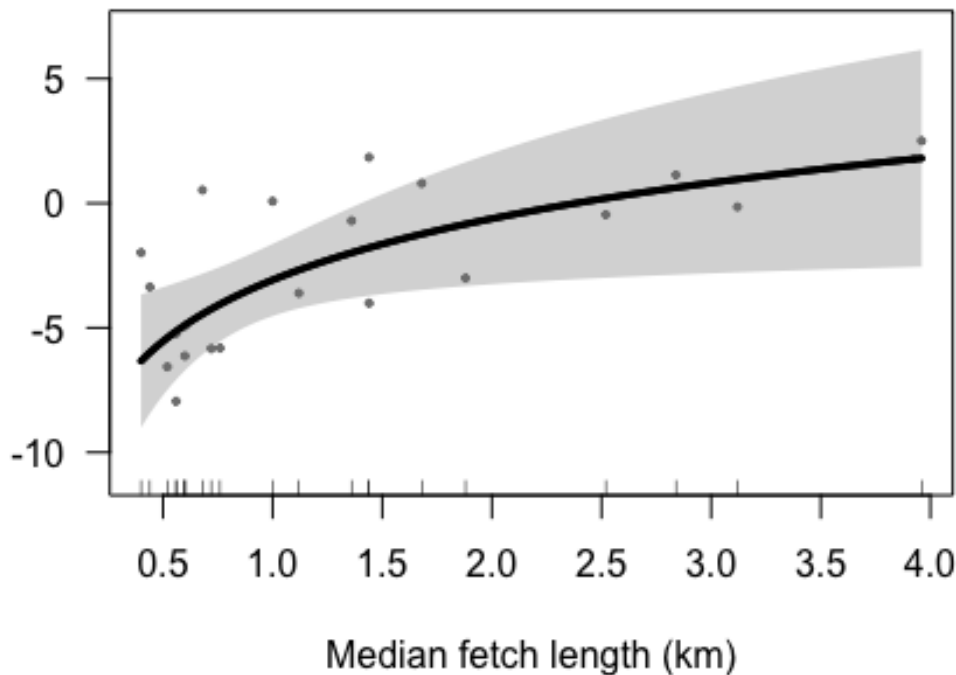


1363

```

1364 visreg(m4, "MedianFetch",
1365         ylim=c(-11, 7),
1366         scale="response",
1367         partial=T,
1368         rug=T,
1369         line=list(col="black"),
1370         xlab="Median fetch length (km)",
1371         ylab="")

```



References

- Baily, B. (2011). Tidal line surveying and Ordnance Survey mapping for coastal geomorphological research. *Survey Review*, 43(321), 252–268. <https://doi.org/10.1179/003962611x13055561708263>
- Baily, B., & Collier, P. (2010). The Development of the Photogrammetric Mapping of tidal lines by the Ordnance Survey. *The Cartographic Journal*, 47(3), 262–269. <https://doi.org/10.1179/000870410x12786821061530>
- Baily, B., & Inkpen, R. (2013). Assessing historical saltmarsh change; an investigation into the reliability of historical saltmarsh mapping using contemporaneous aerial photography and cartographic data. *Journal of Coastal Conservation*, 17(3), 503–514. <https://doi.org/10.1007/s11852-013-0250-7>
- Baily, B., & Pearson, A. W. (2007). Change detection mapping and analysis of salt marsh areas of central southern England from Hurst Castle Spit to Pagham Harbour. *Journal of Coastal Research* 23(6), 1549–1564. <https://doi.org/10.2112/05-0597.1>
- Bridson, R. (1980). Saltmarsh: Its accretion and erosion at Caerlaverock National Nature Reserve, Dumfries. *Transactions of the Dumfriesshire and Galloway Natural History and Antiquarian Society*, 55, 60-67. Retrieved at http://www.dgnhas.org.uk/card_3055-02
- Burd, F. (1992). *Historical study of sites of natural sea wall failures in Essex* (ENRR015). Hull: Natural England. Retrieved from <http://publications.naturalengland.org.uk/publication/33021>
- CCO (Channel Coastal Observatory). (2011). *Annual local monitoring report: Solway Firth*. Allerdale: Allerdale Borough Council. Retrieved from

- 1394 https://www.channelcoast.org/northwest/latest/index.php?link=&dla=download&id=12&cat=1/Solway%20Pages%20from%20Allerdale_Monitoring_Report_2011.pdf
- 1395
- 1396 CH2M HILL. (2013a). *North West Estuaries Processes Reports - Leven Estuary*. Report prepared by
- 1397 CH2M HILL for the North West and North Wales Coastal Group, August 2013. Sefton: Sefton Council.
- 1398 Retrieved from
- 1399 https://www.channelcoast.org/northwest/latest/index.php?link=&dla=download&id=6&cat=1/Leven_Estuary_Processes_Report_Final.pdf
- 1400
- 1401 CH2M HILL. (2013b). *North West Estuaries Processes Reports - Kent Estuary*. Report prepared by
- 1402 CH2M HILL for the North West and North Wales Coastal Group, August 2013. Sefton: Sefton Council.
- 1403 Retrieved from
- 1404 http://www.channelcoast.org/northwest/latest/index.php?link=&dla=download&id=5&cat=1/Kent_Estuary_Processes_Report_Final.pdf
- 1405
- 1406 CH2M HILL. (2013c). *North West Estuaries Processes Reports - Duddon Estuary*. Report prepared by
- 1407 CH2M HILL for the North West and North Wales Coastal Group, August 2013. Sefton: Sefton Council.
- 1408 Retrieved from
- 1409 https://www.channelcoast.org/northwest/latest/index.php?link=&dla=download&id=4&cat=1/Duddon_Estuary_Processes_report_Final.pdf
- 1410
- 1411 Chater, E. H., & Jones, H. (1957). Some observations on *Spartina townsendii* H. and J. Groves in the
- 1412 Dovey estuary. *The Journal of Ecology*, 45(1), 157–167. <https://doi.org/10.2307/2257082>
- 1413
- 1414 Cooper, N. J., Cooper, T., & Burd, F. (2001). 25 years of salt marsh erosion in Essex: Implications for
- 1415 coastal defence and nature conservation. *Journal of Coastal Conservation*, 7(1), 31–40.
- 1416 <https://doi.org/10.1007/bf02742465>
- 1417
- 1418 Dixon-Gough, R. W. (2006). Changes in land use and their implications upon coastal regions: The
- 1419 case of Grange-over-Sands, northwest England. In R. W. Dixon-Gough, P.C. Bloch (Eds.), *The role of the state and individual in sustainable land management, Land Degradation and Development Series* (Vol. 20, Issue 2, pp. 14–31). Aldershot: Ashgate Publishing Ltd.
- 1420
- 1421 FGDC (Federal Geographic Data Committee). (1998). *Geospatial positioning accuracy standards, part 3: National standard for spatial data accuracy* (FGDC-STD-007.3-1998). Washington, DC: U.S.
- 1422 Geological Survey. Retrieved from
- 1423 <https://www.fgdc.gov/standards/projects/accuracy/part3/index.html>
- 1424
- 1425 Firth, C. R., Collins, P. E., & Smith, D. E. (2000). *Focus on firths: Coastal landforms, processes and management options; V: The Solway Firth*. Iselworth: Scottish National Heritage.
- 1426
- 1427 Ganju, N. K., Defne, Z., Kirwan, M. L., Fagherazzi, S., D’Alpaos, A., & Carniello, L. (2017). Spatially
- 1428 integrative metrics reveal hidden vulnerability of microtidal salt marshes. *Nature Communications*, 8, 14156. <https://doi.org/10.1038/ncomms14156>
- 1429
- 1430 Ganju, N. K., Kirwan, M. L., Dickhudt, P. J., Guntenspergen, G. R., Cahoon, D. R., & Kroeger, K. D. (2015). Sediment transport-based metrics of wetland stability. *Geophysical Research Letters*, 42(19), 7992–8000. <https://doi.org/10.1002/2015gl065980>
- 1431
- 1432 Gray, A. J. (1972). The ecology of Morecambe Bay. V. The salt marshes of Morecambe Bay. *The Journal of Applied Ecology*, 9(1), 207–220. <https://doi.org/10.2307/2402057>
- 1433
- 1434 Haynes, T. (2016). *Scottish saltmarsh survey national report* (Commissioned Report No. 786). Inverness: Scottish Natural Heritage. Retrieved from
- 1435 [https://www.nature.scot/sites/default/files/2017-05/Publication%202016%20-](https://www.nature.scot/sites/default/files/2017-05/Publication%202016%20-%20National%20Report.pdf)
- 1436

- 1437 [%20SNH%20Commissioned%20Report%20786%20-](#)
1438 [%20Scottish%20saltmarsh%20survey%20national%20report%20%28A2215730%29.pdf](#)
- 1439 HMLR (Her Majesty's Land Registry). (2016). *HM Land Registry plans: The basis of HM Land Registry*
1440 *applications* (PG40s1) London: Her Majesty's Land Registry. Retrieved from
1441 [www.gov.uk/government/publications/land-registry-plans-the-basis-of-land-registry-](http://www.gov.uk/government/publications/land-registry-plans-the-basis-of-land-registry-applications/land-registry-plans-the-basis-of-land-registry-plans-practice-guide-40-supplement-1)
1442 [applications/land-registry-plans-the-basis-of-land-registry-plans-practice-guide-40-supplement-1](http://www.gov.uk/government/publications/land-registry-plans-the-basis-of-land-registry-plans-practice-guide-40-supplement-1).
- 1443 Jenny, B., & Hurni, L. (2011). Studying cartographic heritage: Analysis and visualization of geometric
1444 distortions. *Computers & Graphics*, 35(2), 402–411. <https://doi.org/10.1016/j.cag.2011.01.005>
- 1445 Jongepier, I., Soens, T., Temmerman, S., & Missiaen, T. (2016). Assessing the planimetric accuracy of
1446 historical maps (sixteenth to nineteenth centuries): New methods and potential for coastal
1447 landscape reconstruction. *The Cartographic Journal*, 53(2), 114–132.
1448 <https://doi.org/10.1179/1743277414y.00000000095>
- 1449 Kestner, F. J. T. (1962). The old coastline of the Wash. *The Geographical Journal*, 128(4), 457–471.
1450 <https://doi.org/10.2307/1792042>
- 1451 Kestner, F. J. T. (1975). The loose-boundary regime of the Wash. *The Geographical Journal*, 141(3),
1452 388–414. <https://doi.org/10.2307/1796474>
- 1453 Kirby, R. (2013). The long-term sedimentary regime of the outer Medway estuary. *Ocean and*
1454 *Coastal Management*, 79, 20–33. <https://doi.org/10.1016/j.ocecoaman.2012.05.028>
- 1455 Kirwan, M. L., Temmerman, S., Skeeahan, E. E., Guntenspergen, G. R., & Fagherazzi, S. (2016).
1456 Overestimation of marsh vulnerability to sea level rise. *Nature Climate Change*, 6(3), 253–260.
1457 <https://doi.org/10.1038/nclimate2909>
- 1458 Manning, A. J., & Whitehouse, R. S. J. (2012). *Enhanced UK estuaries database: Explanatory notes*
1459 *and metadata* (HR Wallingford Report DDY0427 – RT002-R02-00). Wallingford: HR Wallingford.
1460 Retrieved from: <http://eprints.hrwallingford.co.uk/650/1/DDY0427-RT002-R02-00.pdf>
- 1461 Marshall, J. R. (1962). The morphology of the upper Solway salt marshes. *Scottish Geographical*
1462 *Magazine*, 78(2), 81–99. <https://doi.org/10.1080/00369226208735859>
- 1463 Phelan, N., Shaw, A., & Baylis, A. (2011). The extent of saltmarsh in England and Wales: 2006-2009.
1464 Bristol: Environment Agency. Retrieved from [https://www.gov.uk/government/publications/the-](https://www.gov.uk/government/publications/the-extent-of-saltmarsh-in-england-and-wales-2006-to-2009)
1465 [extent-of-saltmarsh-in-england-and-wales-2006-to-2009](https://www.gov.uk/government/publications/the-extent-of-saltmarsh-in-england-and-wales-2006-to-2009)
- 1466 Prandle, D., Lane, A., & Manning, A. J. (2005). Estuaries are not so unique. *Geophysical Research*
1467 *Letters*, 32(23). <https://doi.org/10.1029/2005gl024797>
- 1468 Pringle, A. W. (1995). Erosion of a cyclic saltmarsh in Morecambe Bay, north-west England. *Earth*
1469 *Surface Processes and Landforms*, 20(5), 387–405. <https://doi.org/10.1002/esp.3290200502>
- 1470 Spearman, J., Baugh, J., Feates, N., Dearnaley, M., & Eccles, D. (2014). Small estuary, big port –
1471 progress in the management of the Stour-Orwell estuary system. *Estuarine, Coastal and Shelf*
1472 *Science*, 150, 299–311. <https://doi.org/10.1016/j.ecss.2014.07.003>
- 1473 Wernette, P., Shortridge, A., Lusch, D. P., & Arbogast, A. F. (2017). Accounting for positional
1474 uncertainty in historical shoreline change analysis without ground reference information.
1475 *International Journal of Remote Sensing*, 38(13), 3906–3922.
1476 <https://doi.org/10.1080/01431161.2017.1303218>

- 1477 Wolters, M., Garbutt, A., & Bakker, J. P. (2005). Salt-marsh restoration: Evaluating the success of de-
1478 embankments in north-west Europe. *Biological Conservation*, 123(2), 249–268.
1479 <https://doi.org/10.1016/j.biocon.2004.11.013>
- 1480 Yapp, R. H., Johns, D., & Jones, O. T. (1917). The Salt Marshes of the Dovey Estuary. *The Journal of*
1481 *Ecology*, 5(2), 65. <https://doi.org/10.2307/2255644>
- 1482 Zuur, A. F., Ieno, E. N., Walker, N., Saveliev, A. A., & Smith, G. M. (2009). Mixed effects models and
1483 extensions in ecology with R. New York: Springer NY. <https://doi.org/10.1007/978-0-387-87458-6>
1484
1485